UNIVERSITÀ POLITECNICA DELLE MARCHE

Facoltà di Medicina e Chirurgia

Dipartimento di Scienze Cliniche e Molecolari

PhD Program in Human Health

Cycle XXXII

GENERATION OF HUMAN PDGFRα-TRANSGENIC MOUSE: A NOVEL EXPERIMENTAL MODEL OF SKIN FIBROSIS

Candidate:

Silvia Agarbati

Tutor:

Armando Gabrielli, Prof.

Co-tutor:

Gianluca Moroncini, Prof.

Years 2016/2019

INDEX OF CONTENTS

ABSTRACT

Background: Platelet Derived Growth Factor (PDGF) Receptor α (PDGFRα) is a target of the autoimmune response in scleroderma (SSc). Both total serum IgG (SSc-IgG) and anti-PDGFRα antibodies cloned from memory B cells of SSc patients (SSc-Mabs) [1] demonstrated the ability to increase collagen gene transcription in healthy donor skin fibroblasts and to induce fibrosis *ex vivo,* in skin grafts in SCID mice [2]. In order to replicate these findings *in vivo*, we generated human PDGFRα-transgenic mice.

Materials and Methods: Full length human PDGFRα cDNA was knocked-in into the ubiquitously expressed Rosa26 locus on mouse chromosome 6. Correctly targeted C57BL/6 ES cell clones were selected for blastocyst microinjection, followed by chimera production. F2 heterozygous C57BL/6-hPDGFRα transgenic mice were used to establish the colony. Twelve weeks-old male mice were injected into the back skin at days 0, 3, 6 and 9, either with 0.02 mg/ml of SSc-Mabs (VH_{PAM}-Vκ16F4 or VH_{PAM}-Vκ13B8), or with 2 mg/ml of SSc-IgG or IgG purified from serum of healthy donors (HD-IgG). Vehicle only injection control was included. Age- and sex- matched C57BL/6 wild type mice were used as controls. Animals were sacrificed at day 14. Human PDGFRα transgene expression and collagen amount were assessed in explanted skin tissue. To induce systemic fibrosis, osmotic minipumps containing either 200 µl PBS as vehicle or SSc-MabVH_{PAM}-Vκ16F4 (100 µg) or SSc-MabVH_{PAM}-Vλ16F4 (100 µg) or a combination of SSc-Mabs VH_{PAM}-Vκ16F4 and VH_{PAM}-Vλ16F4 (50 µg + 50 µg) were implanted for 28 days on the back skin of animals. Mice were sacrificed at day 28. Collagen amount, M2 macrophages and alpha smooth muscle (α-SMA) deposition were assessed in explanted skin and lung tissue.

Results: Transgenic mice were phenotypically normal, fertile, and did not display any apparent pathological features.

Human PDGFRα mRNA and protein were detectable in the skin of all examined transgenic mice. Intradermal injection of stimulatory human SSc-Mab VH_{PAM}-Vκ16F4 or SSc-IgG resulted in dermal thickening and increased collagen deposition, whereas non-stimulatory human SSc-Mab VH_{PAM}-Vκ13B8 or HD-IgG did not induce any significant skin tissue alterations compared

to vehicle control. C57BL/6 wild type mice did not show any significant skin tissue changes with any antibodies.

Subcutaneous continuous administration of SSc-MabVH_{PAM}-Vκ16F4 or SSc-MabVH_{PAM}-Vλ16F4 or the combination of SSc-Mabs VH_{PAM}-Vκ16F4 and VH_{PAM}-Vλ16F4 resulted in dermal thickening and increased collagen deposition in skin tissue. Moreover perivascular and peribronchiolar increased collagen amount were detected in lung tissue, with some inflammatory areas characterized by M2 macrophages and α-SMA endothelial positive cells in small vessels.

Conclusions: We generated a novel humanized mouse model of skin fibrosis based on the concomitant expression of human PDGFRα and injection of stimulatory anti-PDGFRα antibodies. This mouse model may be useful for identification and preclinical validation of new therapeutic strategies for SSc.

1 INTRODUCTION and BACKGROUND

1.1. Classification and epidemiology of Systemic Sclerosis

Systemic sclerosis or scleroderma (SSc) is a multisystem connective tissue disease characterized by immune dysregulation, obliterative vasculopathy, and fibrosis of skin and internal organs. It has the highest disease-related mortality and morbidity with an impaired quality of life among the rheumatologic illness [3]. It is believed that its complex pathophysiology involves genetic and environmental factors, vascular and immune system functions, as well as fibroblasts and extracellular matrix alterations. Clinically it is characterized by the massive deposition of collagen fibers in tissues such as the gastrointestinal tract, lungs, heart and kidneys, by alterations of the microvasculature and by disturbances of the immune system at both the cellular and humoral level. Patients with SSc almost universally present numerous autoantibodies, some of which seem to be disease-specific.

The results of studies of the prevalence and incidence of SSc are conflicting because of methodological variations in case ascertainment and geographic differences in these measurements.

The available data indicate a prevalence ranging from 50 to 300 cases per 1 million persons and an incidence ranging from 2.3 to 22.8 cases per 1 million persons per year. Women (age range mainly between 30 and 50 years) are at much higher risk for scleroderma than men, with a ratio ranging from 3:1 to 14:1 [4].

Subsets of SSc can be discerned: limited cutaneous SSc (lcSSc), diffuse cutaneous SSc (dcSSc), and SSc without skin involvement [5].

In limited cutaneous SSc, fibrosis is mainly restricted to the hands, arms, and face. Raynaud's phenomenon is present for several years before fibrosis appears and pulmonary hypertension (PAH) is frequent. The prognosis is significantly more favourable when compared with patients with the diffuse variant. Limited SSc indeed presents a more benign disease course and a lower incidence of renal involvement (Figure 1A).

Diffuse cutaneous SSc is a rapidly progressing disorder that usually begins with symmetric finger and hand swelling that generalizes to involve the forearms, arms, face, trunk, and lower extremities. Over time, the oedema evolves into firm bound-down induration and fibrosis that

eventually cause deformities of the digits, which typically show fixed-flexion contractures of the proximal interphalangeal joints. In the majority of diffuse scleroderma patients, the onset of edema takes place soon after the first episode of Raynaud's phenomenon. In dSSc the internal organ involvement is early and severe and compromises one or more organs. Anti-topoisomerase I antibodies are present in approximately 40% of dSSc patients (Figure 1B).

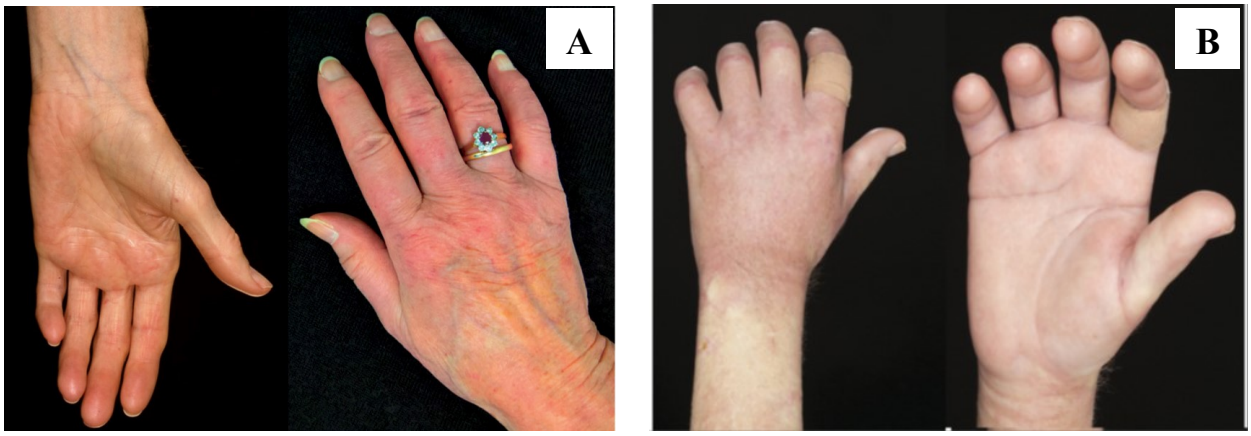

Figure 1. (**A**) **Limited cutaneous systemic sclerosis**. Limited cutaneous SSc is associated with mild skin involvement distal to the elbows and knees, with or without face and neck involvement, and sparing of the chest and abdomen. A representative image of sclerodactyly. (**B**) **Diffuse cutaneous systemic sclerosis**. Hand function is affected in these patients and is often associated with severe digital ulcers and ulceration over areas of pressure or trauma [6].

In the past the term CREST (calcinosis, Raynaud's phenomenon, esophageal motility dysfunction, sclerodactyly, and telangiectasia) syndrome was comprised within the limited scleroderma subset, but it no longer used. A small number (<5%) of patients have clinical features (most commonly Raynaud's phenomenon, digital ulcers, and pulmonary arterial hypertension) and autoantibodies that are specific to systemic sclerosis, but no skin involvement (so-called sine scleroderma). Patients with scleroderma plus evidence of systemic lupus erythematosus, rheumatoid arthritis, polymyositis, or Sjogren's syndrome are considered to have an overlap syndrome. In some patients, organ-based manifestations of the disease are observed, which might include lung fibrosis, pulmonary arterial hypertension, renal failure (usually with accelerate-dphase hypertension and a thrombotic microangiopathy clinical picture), or gastrointestinal complications [6].

The involvement of visceral organs is a major factor in determining the prognosis; severely debilitating esophageal dysfunction is the most common visceral complication, and lung involvement is the leading cause of death [7].

Fibrosis is caused by fibroblast activation, proliferation and increased deposition of extracellular matrix (ECM) proteins such as fibronectin and collagen in various organs. Progression of organ fibrosis leads to end-stage organ failure as a result of the loss of normal structure and function. Notably, interstitial lung disease (ILD) is currently one of the most significant complications of SSc. ILD is currently the leading cause of death in patients with SSc. Furthermore, skin fibrosis causes reduction of wrinkles and disappearance of the cutaneous furrows. These features lead to diminished mouth opening and width, concomitance of sicca syndrome, and finger joint contractures with impaired quality of life [6].

In general, the survival rate lies between 34 and 73% [8]. It is, however, lower and associated with a poorer prognosis in men and older patients, while women and younger patients generally present a higher survival score and better prognosis. In SSc patients, it has also been observed an increased susceptibility to the development of cancer, mainly of the lung [9].

1.2 Pathogenesis of Systemic Sclerosis

SSc is a clinically heterogeneous disease; despite extensive investigations, the key pathogenic links between these disease hallmarks remain obscure, as well as the etiology underlying the beginning of this complex disorder.

Familial clustering of the disease, the high incidence of other autoimmune disorders in families of patients with scleroderma [10], and differences in phenotype among racial and ethnic groups, suggest that genetic factors contribute to SSc. The most prominent genetic factor is gender. Epidemiologic studies have shown a significant increase in the risk of SSc in first-degree relatives of patients with the disease: 1.6% versus a 0.026% risk in the general population, and there is strong evidence of familial clustering of cases [11]. Twin concordance rates for scleroderma are low; in the latest publication to date involving 42 twin pairs, the concordance rate for monozygotic twin pairs was 4.2% and for dizygotic twin pairs 5.6% [12].

Candidate gene association studies and gene linkage studies (GWAS) have clearly indicated both human leukocyte antigen (HLA) and non-HLA genes that are associated with scleroderma, its subphenotypes and its specific autoantibodies.

The HLA gene loci show the strongest association and particularly with specific autoantibodies (e.g. anti-topoisomerase 1 with DPB1*1301, anti-fibrillarin with DRB1*1302). The association

with the non-HLA loci is only modest, but more importantly, these gene associations have implicated a number of immune pathways likely relevant in pathogenesis. These associated genes codes for proteins involved in immune processing, antigen presentation and inflammation, immune signalling, T-cell differentiation and activation, and innate immunity [13] Further, many of these latter genes have also been associated with other known autoimmune disorders (e.g. systemic lupus erythematosus (SLE), thyroid disease, Type 1 diabetes mellitus) [14].

Viral agents have been traditionally considered as potential etiopathogenic triggers of SSc. The most compelling evidences in favor of a viral etiopathogenesis of SSc are focused on cytomegalovirus (CMV) and Parvovirus B19. Chronic CMV infections in humans may play an important role in the pathogenesis of vascular injury that involves small vessels, particularly the arterioles. Along with smooth muscle cells, epithelial cells are the predominant targets for virus CMV replication which might induce epithelial-mesenchymal transition (EMT), a relevant step in fibrosis [15]. Recent studies are focusing on the involvement of adenovirus.

In the pathogenesis of scleroderma play a central role: endothelial damage, excessive production and deposition of collagen involving fibroblasts, oxidative stress and reactive oxygen species (ROS), oxygenation of the tissues, and finally autoimmunity, which reflects the coordinated activation of innate and adaptive immune responses (Figure 2).

Endothelial dysfunction is considered a pivotal factor contributing to peripheral vessel remodelling in SSc. Endothelial-to-mesenchymal Transition (EndoMT) may represent a crucial link between endothelial cells (ECs) dysfunction and development of fibrosis.

EndoMT is a phenotypical conversion in which ECs downregulate the expression of their specific markers, such as CD31/platelet-EC adhesion molecule-1, von Willebrand factor (vWF) and vascular endothelial (VE)-cadherin, and acquire mesenchymal cell products including α-SMA, S100A4/fibroblast-specific protein-1 (FSP1) and type I collagen, together with stabilisation and nuclear translocation of the transcriptional regulator Snail1, a crucial trigger of mesenchymal transition.

Multiple pathways such as transforming growth factor-β (TGFβ), endothelin-1 (ET-1), notch, sonic hedgehog and Wnt pathways may participate in the molecular mechanisms of the EndoMT process.

This evidence was demonstrated by Matucci *et al* in a study involving SSc patients and two mouse models of the disease [16].

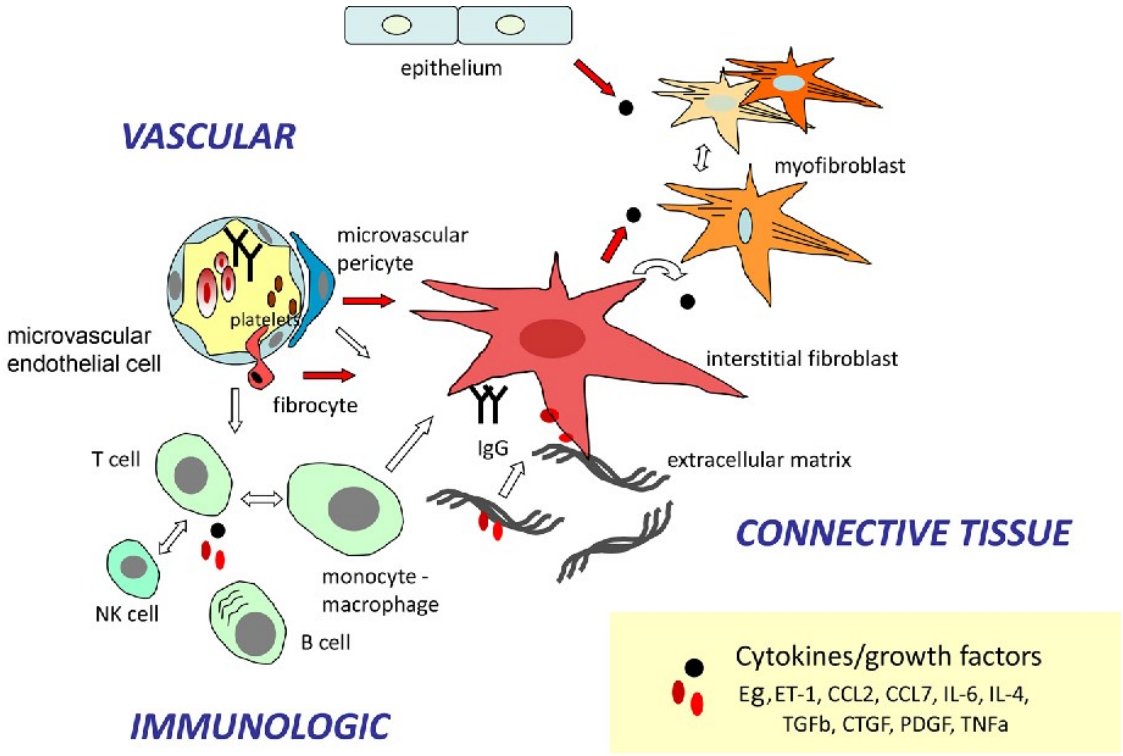

Figure 2. Cellular interplay in the pathogenesis of SSc. CCL2, chemokine ligand 2; CCL7, chemokine ligand 7; CTGF, connective tissue growth factor; ET-1, endothelin-1; IgG, immunoglobulin G; NK, natural killer; PDGF, platelet-derived growth factor; TGFb, transforming growth factor beta; TNFa, tumor necrosis factor alpha [11].

Regarding excessive extracellular-matrix production, Le Roy *et al* provided data demonstrating that *in vitro* the scleroderma fibroblast produces more soluble collagen, synthesizes collagen more rapidly, and fourfold more of its protein synthetic activity is directed to collagen production than in the normal skin fibroblast. Proline hydroxylase levels, an enzyme involved in collagen synthesis, have been variably elevated in skin biopsy material from scleroderma patients [17].

Recent studies have demonstrated that fibroblasts of SSc patients produce, in vitro, high levels of reactive oxygen species (ROS). The resulting oxidative stress induces the activation of fibroblasts, resulting in an increased proliferation rate and augmented transcription of collagen genes. ROS are also able to induce the expression and stabilization of Ras protein, through the activation of extracellular-signal-regulated kinases (ERK1/2) [18]. It is known that the production of ROS can also be triggered by the binding of PDGF to its receptor expressed on the cell surface of fibroblasts, and by the subsequent activation of NADPH oxidase.

Profound alterations characterize the adaptive immune response in systemic sclerosis, and several layers of evidence support a prominent role exerted by immune cellular effectors and humoral mediators in the pathogenesis of this disease. These include (i) the presence of oligoclonal T cells in tissues undergoing fibrosis consistent with (auto)antigen-specific recruitment, (ii) the preferential expansion of polarized CD4+ and CD8+ T cells producing pro-fibrotic cytokines such as IL-4 and IL-13, (iii) the presence of increased number of cells producing mediators belonging to the IL-17 family, including IL-22, which may drive and participate in inflammatory pathways involving epithelial cells as well as fibroblasts, (iv) the deficient or redirected function of T regulatory cells favoring fibrosis, and (v) the enhanced expression of CD19 and CD21 on naïve B cells, and the upregulation of co-stimulatory molecules in mature B cells, which together with the increased levels of B cell activating factor (BAFF) underlie the propensity to an exaggerated humoral response possibly favoring fibrogenesis [19].

T lymphocytes and cytokines

The abundance of CD4+ T lymphocytes in the perivasal infiltrates and in the neo-formed fibrotic tissue, commonly found in scleroderma patients as a result of a generalized state of inflammation, suggests that these cells could hold a pathogenic role in the disease [20]. CD4+ cells constitute the “helper” class of lymphocytes (Th). T lymphocytes of SSc patients show a remarkable increase of the Th2 subset, with consequently increased IL-4, IL-6, IL-10 and IL-13 serum levels. Moreover, the plasmatic level of monocyte chemoattractant protein 1 (MCP-1) is significantly increased during the course of scleroderma, contributing to the unbalance towards the Th2 phenotype. Indeed, MCP-1 is an important pro-fibrotic factor in vitro and it has been shown to regulate the migration of monocytes and Th2 lymphocytes at sites of inflammation [21].

B cells in SSc and fibrosis

Analysis of circulating B cell repertoire in SSc has shown expansion of the (CD27-) naïve B cell subset and the concurrent decline of memory B cells and plasmacellular components.

However, both naive and memory B cells from SSc patients overexpressed a positive response regulators such as CD19; loss of CD19 expression attenuates skin and lung fibrosis in the bleomycin-induced SSc mouse model. Members of the tumor necrosis factor (TNF) superfamily exerting important homeostatic functions on B cells, BAFF (B cell activating factor) and APRIL (a proliferation-inducing ligand), are increased in SSc patients and associated with specific

clinical manifestations such as extent of skin involvement and the presence of pulmonary fibrosis.
In addition, B cells were shown to induce contact-dependent human dermal fibroblasts activation with upregulation of, among other mediators, type I collagen [19].

1.3 Autoantibodies and Systemic Sclerosis

SSc is also characterized by the presence of circulating autoantibodies to several cellular and extracellular components. Around 95% of patients with SSc have detectable autoantibodies, which in most cases are highly specific for the disease. The target antigens for the commonly seen antibodies are all intranuclear.
Distinct specificities of antinuclear antibodies (ANAs) are selectively detected in SSc patients and are associated with unique disease manifestations, but do not have a proven pathogenic role. A new group of autoantibodies reactive with cell surface receptors have been identified in SSc patients. They have been shown to directly activate pathways that may contribute to tissue and vascular damage [22].

1.3.1. Anti-nuclear antibodies (ANA)

One representative feature of the immunological abnormalities in SSc patients is the presence of antinuclear antibodies (ANA). ANA are present in more than 90% of SSc patients, and these ANA react against various intracellular components.
Anti-centromere antibodies (ACA) and anti-topoisomerase I antibodies (anti-topo I, formerly anti-Scl-70) are the classic ANA found in SSc.
Autoimmune disease detection protocol starts with determination of ANA performed through immunofluorescence staining (IF) using HEp-2 cells and a positive ANA test leads to further investigation of extractible nuclear antigens (ENA) [23].
Except for ACA, it is difficult to identify the specific ANA by IF because epitopes cannot be well defined using this technique.
Therefore, additional techniques such as enzyme-linked immunosorbent assay (ELISA), immunodiffusion and immunoprecipitation are required to confirm ANA in a patient's sera.

a) Anti-centromere antibodies (ACA)

Although the frequency of ACA in patients with SSc has been reported to be 20–30% overall, it varies among different ethnic populations. The presence of ACA are predictive for development of pulmonary hypertension but not pulmonary fibrosis [24, 25]. ACA-positive SSc patients possess a more favourable prognosis (associated with limited skin involvement) than patients with other SSc-related ANA [25].

The class of ACA comprises autoantibodies specific for six different centromeric polypeptides (CENP A-F). For clinical use, an ELISA system based on a cloned fusion protein of the CENP-B antigen has been established.

b) Anti-topoisomerase I antibodies

Anti-topo I antibodies were found in approximately 40% of patients with dSSc, but in less than 10% of patients with lSSc. Anti-topo I are usually not found in healthy individuals, in patients with other connective diseases or primary Raynaud's syndrome [26]. They are associated with a higher risk for severe pulmonary fibrosis early in disease.

In vitro studies have revealed direct pathogenic effects of these autoantibodies found in SSc. Henault *et al* [27] have reported that the autoantigen topoisomerase I was bound specifically to fibroblasts, where it was recognized by anti-topo I from SSc patients.

The binding of anti-topo I subsequently stimulated adhesion and activation of cultured monocytes. Topo I released from apoptotic endothelial cells also bound specifically to fibroblasts. Thus, it is possible that, in vivo, topoisomerase I binds to fibroblast surfaces, recruits anti-topo I and subsequently induces monocyte adhesion and activation, leading to the development of SSc.

c) Other anti-extractable nuclear antigens (ENA) antibodies

<u>Anti-RNA polymerase I, II and III antibodies</u>

The co-presence of anti-RNA polymerase RNAP I and III antibodies is specific to SSc with a prevalence of approximately 20% and is usually associated with diffuse cutaneous involvement and higher risk of renal crisis.

Antibodies to RNAP II alone are rare and not specific for SSc because they are also detectable in SLE and overlap syndrome.

Anti-Th/To antibodies (anti-Th/To, known as anti-7-2RNA antibodies)

Anti-Th/To are present in a small subset of patients with SSc (2–5%) and are associated with limited skin involvement, but a high risk for severe organ involvement and therefore they stand for a worse overall prognosis.

Some antinuclear antibodies can be found in SSc-myositis overlap:

✓ Anti-U1RNP antibodies (anti-U1RNP) – found in 90% of patients with mixed connective tissue disease and in approximately 6% of SSc patients.

✓ Anti-RM-Scl (anti-PM-Scl) – found in 4-11% of SSc-myositis overlap patients, but only in 2% of patients with scleroderma only.

1.3.2 Antibodies other than Anti-nuclear antibodies

In SSc patients there is another group of autoantibodies reactive with cell surface receptors. These include the antibodies anti-endothelial cells (AECA), anti-angiotensin II type 1 receptor (AT1R), anti-endothelin-1 type A receptor (ETaR) and a new class of antagonistic autoantibodies, the anti-muscarinic-3 receptor (M3R) antibodies.

- AECA are indicative of the entity of vascular damage and the extent of visceral involvement; these autoantibodies are able to increase in endothelial cells the expression of inflammatory cytokines (IL-1, IL-6 and MCP-1) and adhesion molecules (ICAM-1), thus may contribute to SSc vascular lesions.
- Angiotensin II type 1 receptor and endothelin-1 type A receptor are widely expressed on cells of the vascular system and on immune cells. Anti-AT1R and anti-ETAR antibodies were found in about 85% of SSc patients. Higher levels of anti-AT1R and anti-ETAR antibodies were associated with severe SSc vascular manifestations such as digital ulcers and PAH. In human dermal microvascular endothelial cells these autoantibodies induce ERK1/2 phosphorylation and increased TGFß gene expression; their role were tested also in vivo.
- Autoantibodies against muscarinic-3 receptor (M3R):

  Gastrointestinal (GI) involvement leading to dysmotility is frequent in SSc as a result of disturbance of cholinergic neurotransmission and smooth muscle atrophy, in which stimulation of the muscarinic-3 receptor (M3R) is the principal excitatory mediator of GI. Anti-M3R autoantibodies may lead to failure of the cholinergic neurotransmission and, in turn, result in GI motility dysfunction. Several studies found a high incidence of anti-myenteric neuronal antibodies in the sera of SSc patients with GI symptoms [22].

1.4. Diagnosis of Systemic Sclerosis

The difficulties inherent in diagnosing, screening and treating SSc are due to the complex pathology of the disease, which involves interplay between the immune system, vasculature and components of connective tissue. Therefore, a cross-disciplinary collaboration in the screening and diagnosis of patients is important. There are multiple tools used in clinical practice, such as clinical history and physical examination (RSS - Rodnan skin score to measure the extent of skin fibrosis), laboratory tests (detection of autoantibodies as markers of disease) and instrumental exams (capillaroscopy and exams for internal organ involvement). In the absence of a diagnostic test proving absence or presence for SSc, several sets of classification criteria have been developed.

Because of the insufficient sensitivity of the 1980 criteria and advances in knowledge about SSc, the American College of Rheumatology (ACR) and the European League Against Rheumatism (EULAR) established a new classification criteria for SSc. The experts concluded that `skin thickening of the fingers of both hands that extends proximal to the metacarpophalangeal joints' was sufficient to classify a subject as having SSc. Further, patients with skin thickening sparing the fingers' are classified as not having SSc. The newly developed classification system includes the four items of the 1980 ARA classification criteria as well as the items of the 2001 proposal for classification of SSc by Leroy and Medsger.

There are 7 domains, some have several possible manifestations and each manifestations have a score: Skin thickening of the fingers (Puffy fingers, Sclerodactyly), Finger tip lesions (Digital Tip Ulcers and Finger Tip Pitting Scars), Telangiectasia, Abnormal nailfold capillaries, Pulmonary arterial hypertension and/or Interstitial lung Disease, Raynaud's phenomenon, Scleroderma related antibodies.

The new classification includes the concept of specific serum autoantibodies such as antitopoisomerase I, anti-centromere, and anti-RNA polymerase III. There is the possibility that other SSc autoantibodies such as anti-Th/To, anti-U3 RNP and others may become more widely available. The maximum possible score is 19 and patients who have 9 points or more are classified as having SSc.

The sensitivity and specificity of the new SSc criteria were 0.91 and 0.92 in the validation sample; the new system is more inclusive and also perform well in patients with early disease, meaning a time since diagnosis of 0–3 years [5].

1.5. Raynaud's phenomenon and early diagnosis of Systemic Sclerosis

The most peculiar vascular dysfunction in SSc is the Raynaud's phenomenon. This clinical feature is caused by the dysregulation of the vascular tone of fingers and toes. It is an episodic digital ischemic vasospasm triggered by cold- or emotional-stress leading to a pale and cyanotic skin with a postischemic phase of hyperemia [28].

Raynaud's phenomenon is further divided into primary Raynaud's disease and secondary Raynaud's phenomenon, related to a connective tissue disease. Primary Raynaud's disease is common, with a prevalence of 3% to 5% in the general population, and remains uncomplicated without permanent injury, while 95% of scleroderma patients have Raynaud's phenomenon, often as the first symptom of disease. The incidence of progression from isolated Raynaud's phenomenon to definite SSc is 12,6% [29] and the incidence of progression to any connective tissue disease (CTD) is 13,6% [29, 30].

In SSc, in addition to an imbalance in endothelial signals (for example, an increased release of vasoconstrictive endothelin), other factors, including impaired vasodilatory mechanisms (such as lowering of nitric oxide levels or of endothelial-dependent relaxation factor), enhanced platelet aggregation and reduced neuropeptide levels, contribute to the vasospastic propensity. Other harmful factors, such as toxic factors, proteases (e.g., granzyme 1), lipoperoxides, and anti-endothelial autoantibodies may contribute to this process [31, 32].

The diagnosis of SSc and, consequently, an appropriate therapy are delayed until the appearance of skin involvement and/or clinically detectable internal organ involvement when microvascular remodeling, tissue fibrosis, or atrophy are already irreversible.

In a recent Delphi exercise [33], four signs/symptoms have been identified as necessary for the very early diagnosis of SSc: Raynaud's phenomenon (RP), puffy swollen digits turning into sclerodactyly, antinuclear antibodies and specific SSc antibodies (ACA and anti-topo I antibodies), and abnormal capillaroscopy with scleroderma pattern.

1.6. Therapy of Systemic Sclerosis

At present there is no etiopathogenetic therapy that can cure SSc, but only symptomatic drugs that can control the most common ailments of the disease. The drugs generally used in the treatment of SSc are:

Immunosuppressing medications: (nonsteroidal anti-inflammatory, high-dose corticosteroids, cyclophosphamide in combination with steroids, cyclosporines) have poor efficacy and their use is rationally restricted to forms of scleroderma characterized by a strong inflammatory component, to control joint muscle and tendon pain. Cyclophosphamide is the only disease-modifying drug, since it is approved and effective for active SSc with lung involvement [34].

Symptomatic organ-specific individual SSc patients have variable and different severity of organ involvement. The treatment must be individualized, to minimize the symptoms and to preserve as much as possible the functionality of each organ. Some examples of organ-specific therapy are: analogs of prostacyclin, with vasoactive action, for the treatment of ulcers and pulmonary hypertension, the proton pump inhibitors and prokinetic drugs for reflux esophagitis, blood pressure medications (particularly angiotensin converting enzyme (ACE) inhibitors) for high blood pressure or kidney problems.

Thanks to the advances made in research in recent years new experimental therapies have been adopted, greatly helping to improve the quality and life expectancy of SSc patients. The drugs currently used are [35, 36]:

• Inhibitors of inflammatory pathway: anti CD-20 (Rituximab), blockers of IL-6 receptor (Tocilizumab)

• Anti-fibrotic drugs: tyrosine kinase inhibitors, Imatinib, Desatinib, Nilotinib

• Endothelin receptor antagonists – ENA (Bosentan, Sitaxentan, Ambrisentan)

Some of these drugs, such as rituximab and imatinib are now used in extensive trials and with good patient outcomes, opening new perspectives to the understanding of the disease. Nevertheless research into disease-specific therapies targeting distinct biological pathways is ongoing.

1.7 Platelet-derived growth factor (PDGF)

Fibrosis occurs in all organs and tissues, becomes irreversible with time and further drives loss of tissue function. Various cells types initiate and perpetuate pathological fibrosis by paracrine activation of the principal cellular executors of fibrosis, i.e. stromal mesenchymal cells like fibroblasts, pericytes and myofibroblasts. Multiple pathways are involved in fibrosis, PDGF-signaling being one of the central mediators [37].

PDGF, platelet-derived growth factor, was identified more than three decades ago as a serum growth factor for fibroblasts, smooth muscle cells (SMCs), and glia cells. Moreover, is the major mitogen for connective tissue cells and certain other cell types.
PDGF induces reorganization of the actin filament system and stimulates chemotaxis, i.e., a directed cell movement toward a gradient of PDGF. In vivo, PDGF has important roles during the embryonic development as well as during wound healing. Moreover, its overactivity has been implicated in several pathological conditions [38].

PDGFs act primarily as paracrine growth factors, may also be engaged in autocrine loops in tumors and are generally produced by discrete populations of cells and act locally to drive different cellular responses. Its expression in cultured cells is dynamic and responsive to a variety of stimuli, including hypoxia, thrombin, cytokines, and growth factors, including PDGF itself.
The PDGF family is composed of four different polypeptide chains, the traditional PDGF-A and PDGF-B, and PDGF-C and PDGF-D. The biologically active PDGF protein forms disulphide-bonded dimers, including four homodimers PDGF-AA, PDGF-BB, PDGF-CC and PDGF-DD, and one heterodimer, PDGF-AB. PDGF-A and PDGF-B are processed intracellularly and secreted in their active forms, while PDGF-C and PDGF-D are secreted as latent factors requiring proteolytic activation.
PDGFs exert their biological activities by activating PDGFRα and PDGFRβ, two structurally related tyrosine kinase receptors that encode a transmembrane protein with an extracellular ligand binding domain and an intracellular tyrosine kinase domain. Tyrosine phosphorylation of the receptor itself and other substrates triggers intracellular signaling cascades that are essential for evoking cellular responses such as migration and proliferation.
Several factors induce PDGFR expression, including TGF-β, estrogen, interleukin-1α (IL-1α), basic fibroblast growth factor-2 (FGF-2), tumor necrosis factor-α, and lipopolysaccharide.

PDGF-α and PDGFRα have a broader role in embryogenesis and function at the sites of epithelial–mesenchymal interactions during organogenesis; excessive activity of PDGF has been associated with several human disorders, including atherosclerosis, balloon injury induced restenosis, pulmonary hypertension, organ fibrosis and tumorigenesis [39].

1.7.1 PDGF Receptor (PDGFR)

There are two PDGFR genes (PDGFRα and PDGFRβ), and they reside on chromosome 4 and 5 in humans and 5 and 18 in mice, respectively.

The cellular responses to PDGF signaling include proliferation, survival, migration, and control of differentiation. PDGF receptors are tightly regulated by an auto-inhibitory allosteric conformation resulting in very low basal activity in the absence of ligand.

Aberrant PDGFR signaling has been implicated in diverse fibrotic conditions where fibroblasts proliferate and deposit excessive connective tissue matrix, leading to progressive scarring and organ dysfunction.

To investigate the in vivo consequences of increased PDGFRα signaling and to gain new understanding of the developmental biology of this receptor and the consequences for disease in adulthood, Olson and Soriano created activatable alleles with higher intrinsic kinase activity at the PDGFRα locus; two separate mouse lines were generated for conditional expression of mutant PDGFRα. The developmental phenotypes resulting from either mutation demonstrate an important role for PDGFRα in the balanced expansion of mesenchymal cells during connective tissue development. In adult animals, increased PDGFRα activation also leads to connective tissue hyperplasia and to progressive, chronic fibrosis in many organs [40].

PDGFα and -β receptors are structurally similar and activate overlapping signal transduction pathways including phosphatidylinositol 3 kinase (PI3K), Ras- MAPK, Src family kinases and phospholipase Cγ (PLCγ) resulting in overlapping biological properties in vitro.

The best-known mechanism to activated PDGFRs is the PDGF-mediated (direct) mode of activation in which activated PDGFR tyrosine phosphorylates substrates engages signaling cascades that drive subsequent cellular responses. For instance, both PDGFRα and PDGFRβ autophosphorylate and thereby create a docking sites for SH2 domain-containing proteins such as phosphoinositide 3 kinase (PI3K). The relocalization of PI3K to the plasma membrane increases its access to its lipid substrates and to co-activators such as activated Ras.

There are also PDGF-independent modes to activate PDGFRs, which were first detected in pathological settings. For instance, indirect activation of PDGFRα is driven by growth factors outside of the PDGF family (non-PDGFs).
These non-PDGFs engage their own receptors and thereby trigger an intracellular signaling cascade that enduringly activates monomeric PDGFRα. It was discovered in the context of experimental PVR, where the pathogenesis depends on prolonged activation of PDGFRα. VEGF enables indirect activation of PDGFRα by antagonizing PDGF-dependent activation of PDGFRα; removing VEGF allows PDGF to block the non-PDGFs, which are responsible for indirectly activating PDGFRα and thereby enabling survival of cells displaced into the vitreous [41].

Another mode of activating PDGFRs depends on antibodies against PDGFRα that are present in the serum of patients with scleroderma, and these autoantibodies activate PDGFRs by binding to their extracellular domain. The results in an increased type I collagen expression and the conversion of fibroblasts to myofibrobalsts.

1.7.2 The role of PDGF in Systemic Sclerosis

Excessive activity of PDGF has been associated with several human disorders, including atherosclerosis, balloon injury induced restenosis, pulmonary hypertension, organ fibrosis and tumorigenesis.
There is evidence that PDGF plays an important role in the pathogenesis of SSc.
Similar to other fibrotic disorders, a potentially relevant pathogenic step in SSc is the transdifferentiation of pericytes and local resident fibroblasts into profibrotic myofibroblasts.

- PDGFs and PDGFRs are upregulated in skin lesions in patients with scleroderma and promote myofibroblast activation.

- Cell culture studies show that PDGF-C has a strong mitogenic and migratory effect on human dermal fibroblasts. PDGF-C produced by M2 macrophages induces α-SMA expression in dermal fibroblasts in vitro and might also promote myofibroblast differentiation in skin fibrosis.

- PDGFR-A silencing by siRNA inhibits fibroblast transdifferentiation into myofibroblasts. Two independent studies show, that scleroderma patients exhibited significantly elevated

levels of circulating PDGF-B (8-fold and 2.5- fold, respectively), which might play a role in the systemic vascular dysfunction and fibrotic changes [37].

- Elevated levels of PDGF-A and PDGF-B were found in bronchoalveolar lavage (BAL) fluid obtained from scleroderma patients.

The role of PDGF in oxidative stress

Platelet-derived growth factor (PDGF) is able to regulate the level of expression of the protein Ras through the activation of intracellular signalling pathways involving extracellular-regulated kinases 1 and 2 (ERK1/2) and the modulation of the production of ROS [42].
Fibroblasts are able to constitutively produce high levels of ROS through the activation of the NADPH-oxidase (NOX-1). ROS produced in this manner are able to mediate apoptotic signalling in a direct way; however, through the induction of NF-kB, they can positively modulate the expression of genes characteristic of the inflammatory response [43].

In parallel, ROS can activate the ERK1/2 pathway, which, in turn, can induce the expression of the Ha-Ras gene. The expression of Ras protein is reinforced and stabilized through the activation of Raf-1, which is modulated by ROS- dependent ERK1/2 stimulation. ERK1/2 and ROS are able to stabilize the expression of Ha-Ras even at the post-translational level, inhibiting its proteasome-mediated degradation [42].
The final result of the Ras expression and stabilization is the triggering of a plethora of intracellular signalling pathways leading to a modification of the fibroblast towards a myofibroblastic phenotype, to collagen synthesis regulation and to pro-inflammatory and apoptotic responses [42].
Fibroblasts from scleroderma patients are shown to basally express an increased number of PDGF receptors (induced by the de-regulation of TGF-β levels [44] and an increased activation of the ERK1/2 and ROS pathways.

1.7.3 PDGF/PDGFR in other organ fibrosis

PDGF and its receptor contribute to normal heart development. Deficient or abnormal expression of PDGF and PDGFR genes have a negative impact on cardiac development and function [45].
In skeletal muscle PDGFRα exhibits divergent effects.

At physiological levels, signalling through this receptor promotes muscle development in growing embryos and angiogenesis in regenerating adult muscle.
Both increased PDGF ligand abundance and enhanced PDGFRα pathway activity cause pathological fibrosis.
In mice PDGFRα signalling regulates a population of muscle-resident fibro/adipogenic progenitors (FAPs) that play a supportive role in muscle regeneration but may also cause fibrosis when aberrantly regulated [46].

1.7.4 Anti-PDGF receptor antibodies

A class of autoantibodies targeting cell surface molecules on fibroblasts has been discovered in the serum of SSc patients [43].
These antibodies are able to bind the human PDGF receptor alpha (PDGFRα) and activate an intracellular pathway that involves ERK1/2, NADPH oxidase and Ras, stimulating the production of ROS and inducing collagen gene transcription (Figure 3).
The activation of this signalling cascade by PDGFR-specific autoantibodies ultimately results in widespread oxidative stress.
This could lead fibroblasts to the acquisition of a myofibroblastic phenotype that might account for a persistent profibrotic response with a subsequent formation of foci of inflammation and further spreading of the fibrotic transformation of the connective tissue [47].
In order to confirm the presence of stimulatory anti-PDGFR autoantibodies in SSc, the immune repertoire of one SSc patient was directly investigated by Moroncini *et al.* [1].

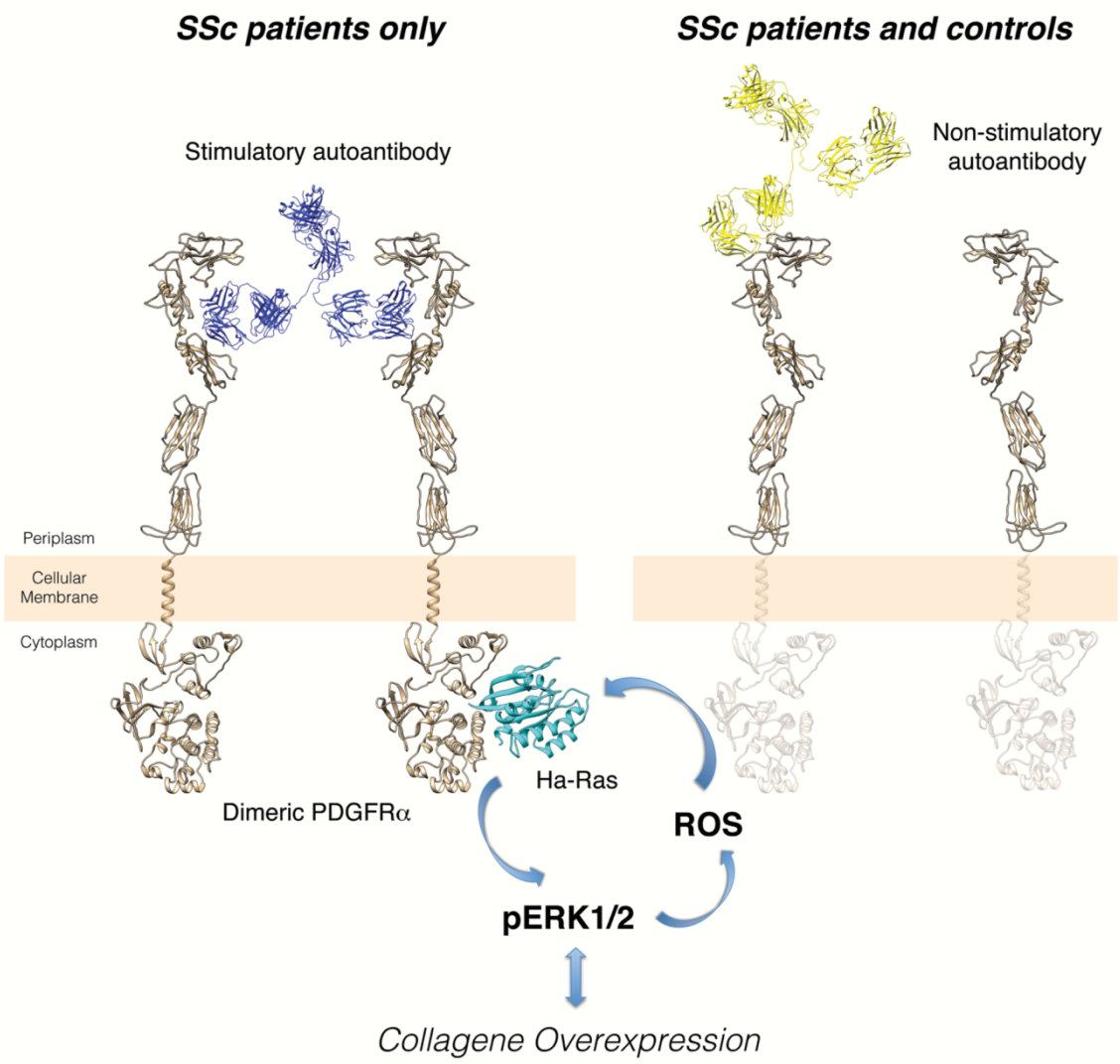

Figure 3. **Distinct epitopes of functional and non functional anti-PDGFRα autoantibodies.**

Left cartoon. Stimulatory autoantibody cloned from memory B cells of a SSc patient binds a discontinuous, conformational epitope of extracellular PDGFRα domain, determining receptor dimerization and subsequent activation of an intracellular signaling loop involving Ha-Ras, phospho-ERK and ROS, inducing collagen gene overexpression. This highlights the importance of this region of PDGFRα as trigger of collagen production in fibroblasts, and identifies possible strategies to block excessive collagen production under pathologic conditions such as SSc.

Right cartoon. Non-stimulatory autoantibody cloned from memory B cells of the same SSc patient binds a single linear epitope of extracellular PDGFRα domain, without subsequent receptor dimerization. This kind of "innocent" autoantibody may reflect the so-called natural autoimmunity, which can be found in many healthy individuals and has no apparent role in physiology nor in disease.[48].

1.7.5. Anti-PDGFRα recombinant human monoclonal autoantibodies

CD22-positive memory B cells were purified by magnetic selection from peripheral blood mononuclear cells (PBMCs) obtained from 1 patient with diffuse SSc; these cells (designated the PAM B cells) were immortalized using Epstein-Barr virus, seeded by limiting dilution in 96-well plates and supernatants of 2,000 wells were screened for the presence of IgG binding to PDGFRα.

Total RNA was extracted from each anti-PDGFRα–positive B cell clone and complementary DNA (cDNA) was amplified with polymerase chain reaction (PCR) primers specific for rearranged human IgG variable region and constant-region heavy- and light-chain genes. Amplified heavy- and light-chain variable regions (VH and VL, respectively) were sequenced; PCR analysis of rearranged IgG genes suggested the presence of a panel of VH and VL chains representative of most IgG subgroups. Upon sequencing, the variable regions of anti-PDGFRα IgG were cloned into an IgG expression vector and the constructs were stably transfected into Chinese hamster ovary (CHO) cells; expression of recombinant IgG in the culture supernatants was confirmed by human IgG–specific enzyme-linked immunosorbent assay (ELISA). Cell cultures were expanded in bioreactor and secreted recombinant human mAb were purified from the supernatants [1].

Later, using a resonant mirror biosensor it was characterized the binding between surface-blocked PDGFRα and PDGFRα-specific recombinant human monoclonal autoantibodies (mAbs) produced by SSc B cells, and it was detected/quantified serum autoimmune IgG with binding characteristics similar to the mAbs [49].

To identify the PDGFRα-specific epitopes of the recombinant human mAb, it was used in silico molecular docking, to predict the binding regions between homology-modeled monomeric human PDGFRα and recombinant human mAb Fab fragments or monomeric human PDGF-BB, the only PDGF isoform with resolved crystal structure. To experimentally validate these predictive data, we screened with PDGF-BB and the recombinant human mAb a conformational PDGFRα peptide library, which was synthesized by Pepscan.

There are 3 distinct PDGFRα epitopes recognized by these antibodies (Figure 4):

- The agonistic recombinant human mAb VH_{PAM}–Vκ16F4 was predicted to bind to a discontinuous epitope within the second and third PDGFRα extracellular domains, largely

overlapping the PDGF-BB binding site. The antibody induce in vitro both ROS and type I collagen genes

- The predicted epitope of the nonagonistic recombinant human mAb VH_{PAM}–Vκ13B8 encompassed a single linear amino acid sequence within the first PDGFRα extracellular domain.
- The larger discontinuous epitope of agonistic recombinant human mAb VH_{PAM}–Vλ16F4 shared part of nonagonistc mAb epitope, which comprised additional amino acid stretches in the first and second PDGFRα domains. The antibody induce in vitro ROS, but not type I collagen genes

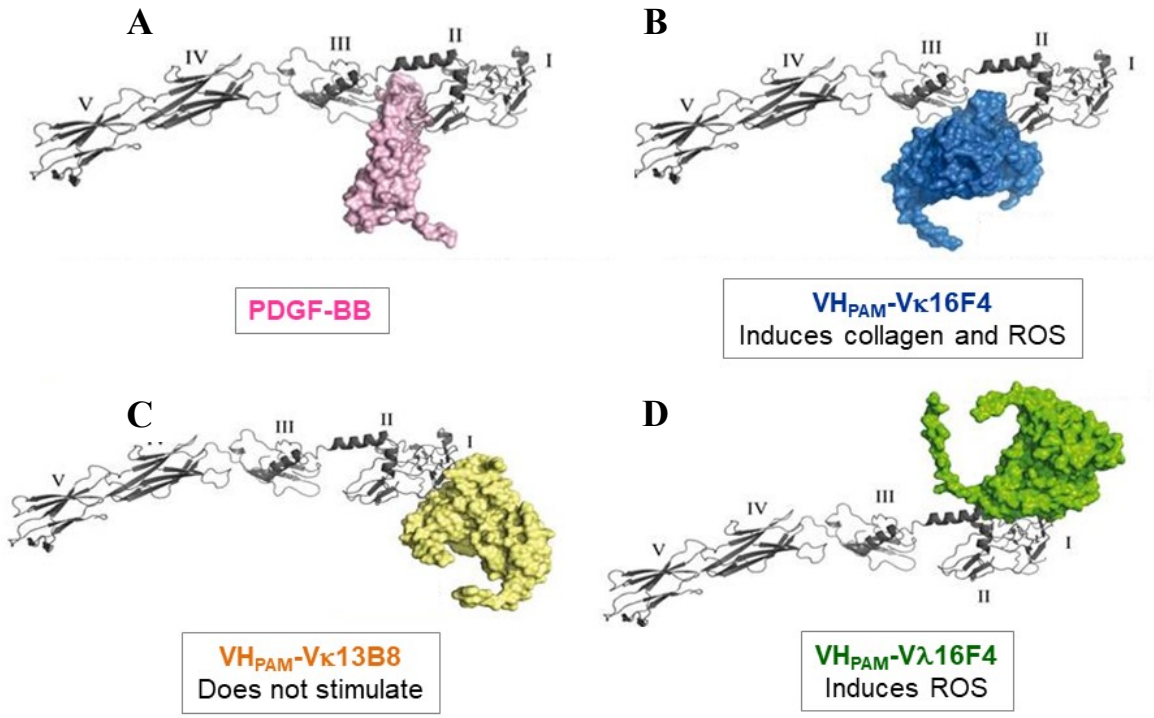

Figure 4. Epitope mapping of human PDGFRα. Molecular docking models show binding of monomeric PDGF-BB **(A)** or Fab fragments of the recombinant human mAb VH_{PAM}–Vk16F4 **(B)**, VH_{PAM}– Vk13B8 **(C)**, and VH_{PAM}–Vλ16F4 **(D)** to the extracellular region of monomeric PDGFRα, encompassing the 5 Ig-like domains (labeled I–V from the N- to the C-terminus).

To detect anti-PDGFRα autoantibodies in the serum of SSc patients three independent assays were established; the first was a direct ELISA with PDGFRα-His immobilized onto 96-well plates by through which it was tested serum samples from 70 consecutive patients with a definite diagnosis of SSc. 94.3% of SSc patients (66 of 70 patients), 48.5% of healthy controls (63 of 130

subjects), and 42.3% of patients with primary RP (11 of 26 patients) were positive for anti-PDGFRα autoantibodies.

Importantly, IgG purified from ELISA-positive SSc serum samples turned out to be positive also in ROS bioassay, whereas IgG purified from ELISA-positive healthy controls serum samples did not.
This indicates, again, that anti-PDGFRα antibodies directed toward non-stimulatory epitopes of the receptor may be present in healthy controls, whereas anti-PDGFRα antibodies directed toward stimulatory epitopes are SSc-specific [1].

Besides confirming the existence of agonistic anti-PDGFRα autoantibodies in SSc patients, it was also mandatory to provide evidence of agonistic activity of these autoantibodies in vivo. The first, indirect evidence came from a small clinical study involving 6 SSc patients with severe skin fibrosis, unresponsive to canonical immunosuppressive therapies, who were treated with 375 mg/m2 per week of rituximab for a total of four doses. The good clinical response observed in all patients, evaluated as decrease of the skin score and improvement of the disability indices, was accompanied by a significant reduction of ROS stimulatory activity in vitro by IgG purified from serum of patients, and downregulation of type I collagen gene expression in fibroblasts grown from skin biopsies [50].

The fibrotic properties of anti-PDGFR agonistic antibodies was demonstrated for the first time *in vivo* using bioengineered skin, containing human keratinocytes and fibroblasts, grafted onto a SCID mouse chimera. The dermis of the skin grafts was then injected either with total IgG purified from serum of SSc patient or healthy controls, either with the agonistic, collagen-inducing anti-PDGFRα monoclonal antibody or with the nonagonistic one. Treatment of animals carrying healthy donor skin grafts with SSc IgG or with agonistic anti-PDGFRα monoclonal antibody resulted in the appearance of a bona fide scleroderma phenotype, as confirmed by increased collagen deposition and fibroblast activation markers [2].

Agonistic anti-PDGFRα autoantibodies may contribute not only to the development of SSc fibrotic lesions but also to the development of the vascular features.
This was recently demonstrated on human pulmonary artery smooth muscle cells (HPASMC) that were exposed to combinatorial human monoclonal anti-PDGFRα autoantibody VH_{PAM}–Vk16F4 and to antibody VH_{PAM}–Vk13B8. HPASMC acquired a synthetic phenotype

characterized by higher growth rate, migratory activity, gene expression of type I collagen α1 chain when stimulated with PDGF and autoantibodies against PDGF receptor, but not with normal IgG.
This phenotypic profile is mediated by increased generation of reactive oxygen species and expression of NOX4 (encoding for NADPH oxidase-4) and mTORC1(mammalian target of rapamycin), the last one as a downstream effector in stimulated HPASMC [51].

1.7 Mouse models of Systemic Sclerosis

Although great efforts have been made in the investigation of the nature of SSc, the pathogenesis of the disease is only partially understood.
Mouse models are powerful tools to explore the pathogenesis of human autoimmune diseases. These models can be categorized into two groups, the group of inducible models, where disease is induced by immunization, transfer of autoimmune components or environmental factors and the group of spontaneous models (Figure 5), where mice develop disease due to the genetic mutations or modifications without further experimental manipulations. So far, more than twenty different mouse models for SSc have been established, each of which resembles at least one hallmark of SSc. While some disease processes have been already investigated in classical mouse models like the bleomycin-induced model or the TGF-β transgenic mouse model, novel models established in the recent years provide exciting new insights in the pathogenesis of SSc.

1.8.1 Spontaneous models

1.8.1.1 *Fli-1 deficient mice*

Friend leukemia virus integration1 (Fli-1) is a member of the family of Ets transcription factors.
It has been shown that Fli1 acts as a potent repressor of the type 1 collagen gene and thus regulate fibrogenesis. As compared to healthy controls, the level of Fli1 is constitutively suppressed in dermal fibroblasts, dermal microvascular endothelial cells, and keratinocytes of SSc patients, suggesting that Fli1 could play a role in the pathogenesis of SSc.
Various Fli-1 deficient mice have been generated to explore the function of this factor. Target disruption of Fli-1 is a lethal mutation and Fli−/− mice die in uteri; mice with a homozygous

deletion of the C-terminal transcriptional activation (CTA) domain of the Fli1 gene are viable and develop prominent fibrosis in skin. Heterozygous Fli1+/− mice show a more prominent fibrosis in the bleomycin-induced mouse model of SSc. Besides Fli1, a second transcription factor, Krüppel-like factor 5 (Klf5) was also found to be suppressed in dermal fibroblasts of SSc patients; Fli1+/−/Klf5+/− double heterozygous mice spontaneously develop three hallmarks of SSc, including autoimmunity, vasculopathy and tissue fibrosis.

To better explore the role of Fli1 in the disorder, cell-specific conditional Fli1 knockout mice have been generated and investigated. As compared to littermate controls, endothelial cell specific Fli-1 CKO mice showed disorganized dermal microvascular network with significantly compromised vessel integrity, increased vessel permeability, impaired development of basement membrane as well as decreased number of α- smooth muscle actin-positive cells. K14Cre;fl/fl mice, means mice with a conditional depletion of Fli-1, develop autoantibodies against nuclear autoantigens (ANA). Moreover, serum concentrations of IL-4, IL-6 and IL-17, which are key cytokines in SSc pathogenesis, are significantly increased in these mice. The skin of K14Cre;fl/fl mice is characterized by a thickened dermis, densely packed collagen bundles, and perivascular infiltration of T cells, macrophages, and mast cells. Consistently, fibrosis accompanied by prominent pulmonary infiltrates of T and B cells was also found in the lung of these mice [52].

1.8.1.2 *uPAR KO mice*

Urokinase-type plasminogen activator receptor (uPAR), a key component of the fibrinolytic system involved in extracellular matrix remodeling and angiogenesis is expressed on several cells, including endothelial cells, fibroblasts, myofibroblasts as well as immune cells (monocytes, neutrophils and activated T cells). Upon binding to uPAR, the ligand uPA (urokinase) promotes ECM remodeling either directly by converting plasminogen into plasmin or indirectly by activating matrix metalloproteinases [53].
Previous studies have shown that a dramatic decrease of uPAR in SSc patient is associated with vascular disorders and excessive production of extracellular matrix (ECM). In 2014, Manetti *et al*. generated uPAR deficient mice to investigate whether uPAR gene inactivation could result in clinical phenotypes resembling human SSc, such as dermal fibrosis featured by thickening of the dermis, elevated collagen contents, increased number of myofibroblasts and high levels of profibrotic cytokines [54].

1.8.1.3 *SIRT 3 KO mice*

Sirtuin 3 (SIRT3) is a mitochondria-localized deacetylase, which belongs to the highly conserved family of Sirtuins which occupies a central role among the group of molecular regulators of aging processes. Activation of SIRT3 has been implicated in counteracting oxidative stress, defending cells against apoptosis, and preventing cell aging.
Since SSc patients develop disease symptoms generally at later stages of life and certain disease features can be diagnosed with high incidence only in elder patients, the association between aging and pathogenesis of SSc has been implied. It has been shown that SIRT3 expression in skin and lung of SSc patients is reduced as compared to controls. The key role of SIRT3 in tissue fibrosis was confirmed recently in SIRT3-deficient mice; aged mice of this strain develop tissue fibrosis in multiple organs, including lung, heart and kidney.

1.8.1.4 *VEGF transgenic mice*

Vascular endothelial growth factor (VEGF) is a potent proangiogenic molecule. It has been reported that levels of VEGF are strongly increased in sera and skin biopsies in SSc patients across different disease stages pronounced especially in diffuse cutaneous SSc.
To investigate the role of VEGF in SSC, Maurer and colleagues generated transgenic mice overexpressing VEGF (VEGF tg mice), that develop spontaneously significant skin fibrosis and proliferative vasculopathy, two main features of SSc. Furthermore, the profibrotic effect of VEGF was confirmed in two further SSc mouse models where transgenic mice display more pronounced dermal fibrosis than wildtype control mice. In addition, data derived from experiments in vitro revealed a direct stimulatory effect of VEGF on the collagen production by dermal fibroblasts, suggesting that VEGF acts as a profibrotic molecule via direct activation of fibroblasts.

1.8.1.5 *PTEN KO mice*

The protein phosphatase and tensin homolog (PTEN), a dual-specific lipid and protein phosphatase, is known as a tumor suppressor. In SSc patients PTEN expression is reduced and fibroblast specific PTEN KO mice develop fibrosis spontaneously in skin and lung, resembling fibrotic feature of SSc [52].

1.8.1.6 *TIGHT SKIN-1 (TSK-1) and TIGHT SKIN-2 (TSK-2) mice*

Tsk-1 mice are a spontaneously developed strain with a mutation of the fibrillin-1 gene whereas Tsk-2 mutants are generated by administration of the mutagenic agent ethylnitrosourea.
Heterozygous Tsk-1 and Tsk-2 mice spontaneously develop SSc-like features with skin fibrosis and autoimmunity. However, in contrast with SSc, skin fibrosis occurs in hypodermis and pulmonary involvement is characterized by emphysema-like alterations with little fibrosis in these strains. Tsk-1 and Tsk-2 mice also lack typical features of vasculopathy, for example endothelial cell apoptosis.

1.8.1.7 *Fra-2 Transgenic mice*

Fos-related antigen 2 (Fra-2) composed a dimeric transcription factor AP-1; Fra-2 expression is elevated in endothelial cells (ECs) and vascular smooth muscle cells (vSMCs) of the lesional skin of human SSc and in lung. Similar to the sequential pathological processes in the skin, Fra-2 tg mice develop pulmonary arterial occlusion at the age of 12 weeks and pulmonary fibrosis subsequently in another few weeks [55].

1.8.1.8 *Caveolin 1-/- mice*

Caveolins are the coating proteins of caveolae; caveolin 1–dependent internalization of TGFβRs reduces TGF-β signaling through increased receptor complex degradation. Caveolin 1–knockout in mice (caveolin 1-/-) induced a systemic fibrotic disease affecting the lungs and other organs. At the age of 12 weeks, caveolin 1-/- mice show profound alterations in the alveolar septae of the lungs, with replacement of the normal alveolar bilayer lining by abundant ECM. In addition to lung fibrosis, caveolin 1-/- mice develop skin fibrosis with a marked increase in collagen deposition. Caveolin 1 -/- mice also display vascular changes with altered vessel tone and permeability.

1.8.1.9 *Mouse model with selective overexpression of CTGF in fibroblasts*

In the repertory of genetic mouse models, stimulation of any profibrotic or inhibition of any antifibrotic pathway by transgenic or knockout techniques in mice could result in a systemic fibrotic phenotype mimicking human SSc.

The connective tissue growth factor CTGF is a target gene of TGF-β and partially modulate the pro-fibrotic effects of TGF-β. Mouse model with selective overexpression of CTGF in fibroblast displays accelerated tissue fibrosis affecting the skin, lungs, and kidneys. In addition, *Col1a2-CTGF* mice mimic certain aspects of SSc vasculopathy, with progressive blood vessel obliteration [56].

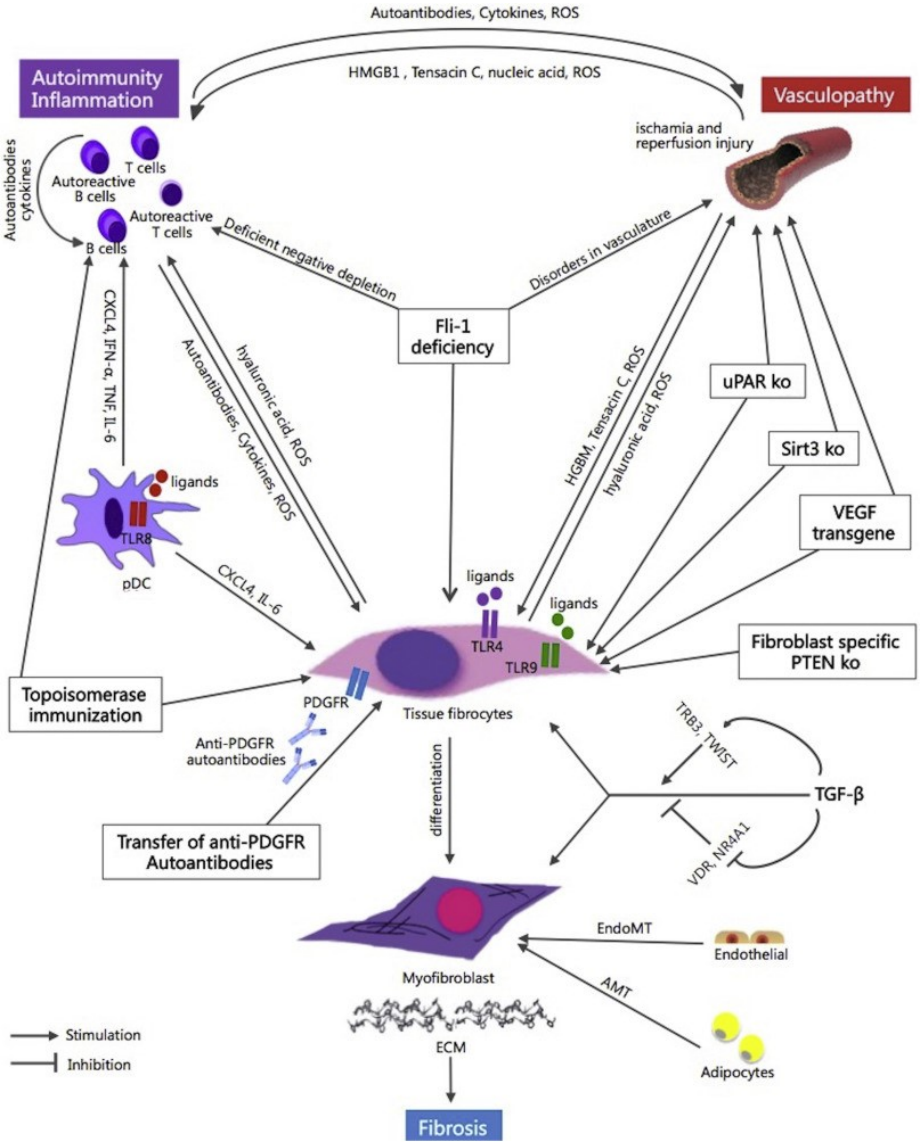

Figure 5. **Summary of the recent advances in pathogenesis of murine models for SSc**. Novel murine models for SSc are indicated as open rectangles, and their contributions to the autoimmunity, fibrosis and vasculopathy are indicated by arrows. Molecules which play an essential role in the pathogenesis of murine models for SSc are depicted in the figure. EndoMT: endothelial cells mesenchymal transition; EMT: epithelial cells mesenchymal transition; AMT: adipocytic cells mesenchymal transition [52].

1.8.1.10 *Transgenic mice for Wnt-10b*

Recent observations provide evidence for the potential importance of Wnts in the development of fibrosis. Wnt10b is a canonical Wnt with potent effects on the regulation of adipogenesis and osteoblastogenesis. Transgenic mice in which Wnt10b is expressed from the fatty acid binding protein-4 (FABP4) promoter showed greatly reduced adipose tissues, resistance to diet-induced obesity and cold intolerance. It was incidentally observed that the transgenic mice have an increase in dermal thickness with a reduced number of adipocytes in the skin. Additional observations provide further evidence linking altered Wnt signaling and cutaneous fibrosis. Moreover, analysis of skin biopsies from patients with SSc revealed altered expression of Wnts and their regulators [57].

1.8.2 Induced models

Bleomycin is a chemotherapeutic antibiotic and its use in animal models of fibrosis is based on the fact that fibrosis is one of the major adverse drug effects of bleomycin in human cancer therapy. Bleomycin it has become associated with two models that have become a cornerstone of experimental fibrosis research. Fibrosis only occurs in certain susceptible mouse strains and the basis of this susceptibility is genetically defined. Several other factors, like gender and age may modify the response to bleomycin.

a) Bleomycin-induced lung fibrosis

The bleomycin-induced lung fibrosis mouse model is representative of many different disorders, ranging from idiopathic pulmonary fibrosis to connective tissue diseases.
Bleomycin can be given by intravenous, intraperitoneal, subcutaneous, or intratracheal routes to initiate lung fibrosis. Intratracheal delivery of bleomycin causes lung damage through direct DNA strand breakage and generation of free radicals inducing oxidative stress. Cell necrosis and apoptosis follows, with subsequent inflammation and the development of fibrosis. Intravenous administration of bleomycin leads to endothelial injury followed by epithelial cell injury, inflammation and fibrosis. The mechanisms for bleomycin-induced tissue injury and fibrosis are complex, including a variety of profibrotic mediators including the stem-cell pathways Wnt, Notch, Hedgehog; transforming growth factor beta (TGF-β), innate immune such as IL-1, IL-6.

Dependent on the route of administration, bleomycin can induce different fibrotic patterns. Intratracheal instillation of bleomycin (Figure 6) results in bronchial concentrically accentuated fibrosis similar with idiopathic pulmonary; a direct instillation of bleomycin into the mouse trachea allowed a rapid diffusion down to the lungs, resulting in extensive inflammation, progressive fibrosis, and a distortion of their normal architecture [58].

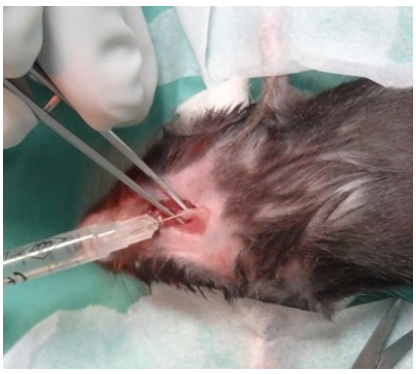

Figure 6. Mice received an endotracheal injection of bleomycin to induce lung injury [59].

b) Bleomycin-induced skin fibrosis

The model of bleomycin-induced skin fibrosis has been very widely used to explore candidate therapies for SSc that may address the inflammatory as well as the fibrotic phase of the disease.
After administration of high doses of subcutaneous bleomycin, systemic manifestations can be seen such as lung fibrosis or the presence of autoimmune antibodies. One of the advantages of this model is that it can be used in various genetically manipulated mice to explore the relationship between inflammatory and fibrotic pathways [60].

1.8.2.1 *Other models of reactive oxygen species in SSc*

Reactive oxygen species have been implicated in the pathogenesis of SSc. A recently described model is induced by daily intradermal injection of hypochlorous acid (HOCl), which causes generation of hydroxyl radicals leading to increased synthesis of collagen in the skin and lung tissue, and anti-DNA topoisomerase 1 antibodies.

1.8.2.2 *Chronic sclerodermatous graft-versus-host disease (cGVHD) model*

Chronic GVHD occurs in 40–60% of long-term survivors after hematopoietic cell transplantation and is the single major factor determining the long-term outcome.
Cytotoxic GVHD and sclerodermatous GVHD are the 2 major forms of chronic GVHD; the fibrosing variant, sclerodermatous GVHD, resembles diffuse SSc. Based on clinical similarities of sclerodermatous GVHD and SSc, transplantation of minor histocompatibility antigens from donor into recipient mice was established as another model that mimics SSc. There are 2

approaches to induce sclerodermatous GVHD in mice that differ in terms of conditioning of recipient mice prior to transplantation: hematopoietic cells can be transplanted in either sub-lethally irradiated BALB/c mice (standard sclerodermatous GVHD model) or immunodeficient recombinase-activating gene 2 (RAG-2) mice (modified sclerodermatous GVHD model). Therefore, reconstitution of hematopoiesis induces sclerodermatous GVHD with inflammation and tissue fibrosis. In the standard sclerodermatous GVHD model spleen as well as bone marrow cells from donor mice are injected into the tail veins of sub-lethally irradiated BALB/c recipient mice. Three weeks after bone marrow transplantation, sclerodermatous GVHD mice develop pulmonary and dermal fibrosis with loss of dermal fat and atrophy of appendages. Alternatively, the same mouse model can be generated transplanting spleen cells from donor mice into immunodeficient RAG-2 recipient mice.
Although a direct comparison of both sclerodermatous GVHD models does not exist, disease manifestations with severe fibrosis of the skin and most internal organs are similar. Autoantibody formation against nuclear antigens occurs in both sclerodermatous GVHD models but might involve different antigen specificities.

1.8.2.3 *Genetic models of SSc induced by selective activation of individual pathogenic signaling pathways*

TGF-ß-mediated model of fibrosis

TGF-β is known as a central profibrotic mediator; incubation of normal fibroblasts with TGF-β induces a SSc-like profibrotic phenotype. Two mouse models have been commonly used to study
the role of TGF-β signaling in vivo.
Expression of a mutated, constitutively active form of the type I TGF-β receptor (TGF-βRICA) enables sustained ligand-independent activation of TGF-β signaling. Two different strategies are currently employed to overexpress TGF-βRICA: a genetic strategy with fibroblast-specific overexpression of TGF-βRICA and overexpression with vectors such as adeno-associated viruses. Challenged mice demonstrate severe skin fibrosis and abnormalities in multiple organs, but do not develop significant pulmonary fibrosis spontaneously.

Another mouse model with aberrant TGF-β signaling was developed by fibroblast-specific overexpression of a non-signaling mutant type II TGF-β receptor using the same promoter

constructs as in TGFβRICA mice lacking in the intracellular kinase domain. Adult transgenic mice develop dermal and pulmonary fibrosis, revealing patchy areas of fibrosis [60].

1.8.2.4 *DNA Topoisomerase I immunized mice*

Autoantibodies directed against DNA topoisomerase I (Topo I) serve as diagnostic marker for SSc and their levels are positively correlated with disease severity. Because of the role of those autoimmunity *against* anti-Topo I may contribute to the pathogenesis of SSc, Hu *et al*. investigated whether immunization with Topo I could induce a SSc-like disease in mice by applying recombinant human Topo I dissolved in complete Freund's adjuvant to four common inbred mouse strains.

Yoshizaki and colleagues reported that immunization with recombinant human Topo I induces a SSc-like disease in C57BL/6 mice, such as tissue fibrosis in the skin and the lung which is accompanied by extensive inflammatory infiltration and alveolar epithelial apoptosis.

Since the antigen used in this SSc model was the entire recombinant Topo I protein, the specific pathogenic epitopes remained unclear. To get more insights into this issue, Mehta and colleagues investigated the pathogenicity of two Topo I-derived peptides, TOPOIA (17 amino acids) and TOPOIB (15 amino acids). After transfer of TOPOIA loaded DC, the mice exhibited high level of anti-Topo I autoantibodies, inflammation and fibrosis in skin and lung, which resembles disease features of SSc [52]

1.8.2.5 *Skin–SCID mouse chimeric model of systemic sclerosis*

Human dermal fibroblasts isolated from skin biopsy specimens from SSc patients can be cultured in vitro and grown as monolayers onto plastic surfaces, where they retain SSc-like features. Keratinocytes and fibroblasts were isolated from forearm skin biopsy specimens from 3 SSc patients and 3 healthy controls, cultured in vitro, and assembled into 3-D bioengineered skins for each donor, which were then independently grafted onto the back of a corresponding number of immunodeficient mice.

Skin humanized mice produced after grafting of bioengineered skin from healthy donors were injected, starting 8 weeks after grafting, with 20 μg of purified serum IgG from a pool of SSc patients or from a pool of healthy controls, or with PBS. Mice injected with SSc IgG displayed significant dermal collagen. Moreover, Luchetti *et al* demonstrated that SSc IgG induce dermal

fibrosis in vivo through PDGFR signaling; to verify that, normal human fibroblasts depleted of both PDGFRα and PDGFRβ were prepared from healthy donors.

These modified fibroblasts impaired the formation of the bioengineered skin, because the human fibroblasts with PDGFR knockdown were unable to sustain a stable keratinocyte/ fibroblast scaffold in vitro [2].

2 AIM OF THE STUDY

Systemic sclerosis (SSc) is a devastating chronic autoimmune disease associated with high impact on the quality and expectation of patients' life.

The identification, in the serum of scleroderma patients, of agonistic autoantibodies targeting PDGFRα and involved in the broad spectrum of pathophysiology, gain the possibility to explore novel therapeutic approaches for this disorder.

In fact, SSc is a drug-orphan connective tissue disease and up to now, unfortunately, no therapeutic strategies are able to totally cure the disease; there are only therapies that can limit specific organ-involvement (for instance pulmonary involvement), but their beneficial effect seems to be short lived and associated with significant side effects.

Considering that autoimmunity play a central role in the pathogenesis of scleroderma, several studies have been focalized on immunological mediators. In this context, PDGF receptor has been identified as one of the target of autoimmune response [43].

It was demonstrated that human anti-PDGFRα monoclonal antibodies cloned from memory B cells of SSC patients are able to induce an increased collagen gene transcription both *in vitro* on fibroblast of healthy donors and *in vivo* on three-dimensional bioengineered human skin grafted onto the back of SCID mice [51][2].

Based on these evidence, it is mandatory to explore and to characterize *in vivo* the pathogenetic mechanisms of these autoantibodies in a immunocompetent and transgenic mouse for human PDGFRα.

Moreover, the availability of an animal model that mimics the typical features of the human disease is essential for studying that disorder.

So, the aim of this study was to obtain a novel mouse model of systemic sclerosis through:

i) the generation of a mouse with ubiquitous expression of human PDGFRα

ii) the induction of skin fibrosis by intradermal injection of human PDGFRα antibodies

iii) the induction of systemic fibrosis by continuous subcutaneous administration of the aforementioned autoantibodies in this transgenic mouse model

3 MATERIALS AND METHODS

3.1 Vector Design and ES Cell Targeting

Full length hPDGFRα cDNA was knocked-in into the ubiquitously expressed Rosa26 locus on mouse chromosome 6. In the Rosa26 targeting vector hPDGFRα cDNA was cloned downstream of the strong synthetic CMV early enhancer/chicken β-actin (CAG) promoter and followed by a polyadenylation (polyA) sequence (Figure 7). Moreover hPDGFRα was linked through an IRES sequence to the green fluorescent protein (GFP) gene, as a reporter for transgene expression. The knock-in vector also carried a loxP flanked expression cassette with a neomycin (Neo) selectable marker, and a diphtheria toxin expression cassette (DTA) for negative selection in ES cells. Rosa26 homology arms were generated by PCR using BAC clones from the C57BL/6J library as template.

C57BL/6 ES cells were used for gene targeting. Correctly targeted ES clones were confirmed by Southern Blotting, then selected for blastocyst microinjection, followed by chimera production. Founders were confirmed as germline transmitted via crossbreeding with Cre delete [40, 61].

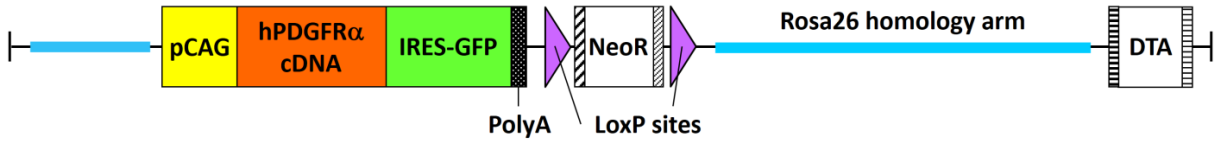

Figure 7. Rosa26-hPDGFRα knock-in vector. Full length hPDGFRα cDNA was knocked-in into the ubiquitously expressed Rosa26 *locus* on mouse chromosome 6. In the Rosa26 targeting vector hPDGFRα cDNA was cloned downstream of the strong synthetic CAG promoter and followed by a polyadenylation (PolyA) sequence. Moreover hPDGFRα was linked through an IRES sequence to the green fluorescent protein (GFP) gene, as a reporter for transgene expression. The knock-in vector also carried a loxP flanked expression cassette with a neomycin (NeoR) selectable marker, and a diphtheria toxin expression cassette (DTA) for negative selection in ES cells.

3.2 Transgenic mouse colony generation

F2 heterozygous C57BL/6-hPDGFRα mice were used to set the new transgenic colony.

Animals were bred as a closed colony and mated only with the C57BL/6 mouse strain to maintain the genetic background [62].

Mice were housed 6 per cage under pathogen-free conditions at Servizio di Allevamento e Sperimentazione Animale I.N.R.C.A., Ancona, Italy, and were maintained under constant temperature and humidity on a 12 h light/dark cycle, with water and standard pellet food *ad libitum* [59]. All animal care and experimental procedures were approved by the Italian Ministry of Health (authorization n. 634/2019-PR) and performed according to the Declaration of Helsinki conventions. Any possible efforts were made to minimize animal suffering [58].

Starting from F2 generation and for a minimum of the next two of them, animal welfare of C57BL/6-hPDGFRα transgenic mice was evaluated in at least 7 male and 7 female puppies coming from different litters. Mice were monitored at birth, at weaning, upon reaching sexual maturity and at subsequent time points. General aspect and morphology, presence of malformations, normal size and weight, growing rate, fertility and litter size, fur appearance, correct posture and motility, behavior and interaction with the environment, together with any clinical or pathological features were observed. Collected data were compared with those obtained from C57BL/6 wild type mice.

3.3 Mouse genotyping

Mouse genotyping was performed by polymerase chain reaction (PCR) on genomic DNA extracted from mouse tail biopsies, using KAPA Mouse Genotyping Kit (KAPA Biosystems) and according to manufacturer's instructions. Specific primer pairs were designed to amplify four different regions of the knocked-in allele (Figure 8), in order to confirm correct genetic transmission of the entire hPDGFRα expression cassette:

Region1 forward 5'-GTTCGGCTTCTGGCGTGTGA-3'; Region1 reverse, 5'-AAGCTGGCAGAGGATTAGGCTCA-3';

Region2 forward, 5'-TCTGAGTTGTTATCAGTAAGGGAGCT-3'; Region2 reverse, 5'-TGTCGCAAATTAACTGTGAATCAT-3';

Region3 forward, 5'-GAACAGACACAGCTCGCAGACCTC-3'; Region3 reverse, 5'-AACGCACACCGGCCTTATTCCA-3';

Region4 forward, 5'-ATCACATGGTCCTGCTGGAGTTC-3'; Region4 reverse, 5'-GGATATGAAGTACTGGGCTCTT-3'.

Rosa26-hPDGFRα knocked-in allele expected fragment size was 383 bp for Region1, 382 bp for Region2, 312 bp for Region3 and 791 bp for Region4. An additional primer pair was used to amplify the Rosa26 wild type allele (i.e. to distinguish between eterozygous and homozygous transgenic mice): Rosa26 forward, 5'-TCAGTAAGGGAGCTGCAGTGGAGT-3'; Rosa26 reverse, 5'-GGAGCGGGAGAAATGGATATGAA-3'. Rosa26 wild type allele expected fragment size was 583 bp.

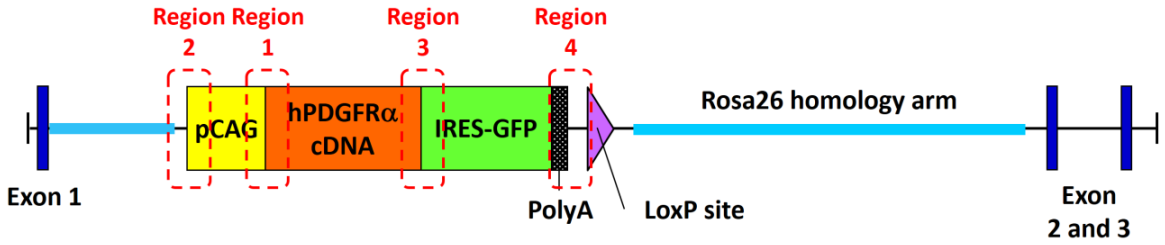

Figure 8. Schematic of mouse genotyping strategy. Specific primer pairs designed to amplify four different regions (region 1, 2, 3, 4 marked with red dotted line) of the knocked-in allele.

Mouse genotyping was performed by polymerase chain reaction (PCR) on genomic DNA extracted from mouse tail biopsies, using KAPA Mouse Genotyping Kit (KAPA Biosystems) and according to manufacturer's instructions. Specific primer pairs were designed to amplify four different regions of the knocked-in allele (Figure 8), in order to confirm correct genetic transmission of the entire hPDGFRα expression cassette:

Region1 forward 5'-GTTCGGCTTCTGGCGTGTGA-3'; Region1 reverse, 5'-AAGCTGGCAGAGGATTAGGCTCA-3';

Region2 forward, 5'-TCTGAGTTGTTATCAGTAAGGGAGCT-3'; Region2 reverse, 5'-TGTCGCAAATTAACTGTGAATCAT-3';

Region3 forward, 5'-GAACAGACACAGCTCGCAGACCTC-3'; Region3 reverse, 5'-AACGCACACCGGCCTTATTCCA-3';

Region4 forward, 5'-ATCACATGGTCCTGCTGGAGTTC-3'; Region4 reverse, 5'-GGATATGAAGTACTGGGCTCTT-3'.

An additional primer pair was used to distinguish between Rosa26 wild type and knocked-in allele (i.e. eterozygous vs. homozygous transgenic mice):

Rosa26 forward, 5'-TCAGTAAGGGAGCTGCAGTGGAGT-3'; Rosa26 reverse, 5'-GGAGCGGGAGAAATGGATATGAA-3'.

3.4 Lifespan analysis of transgenic mice

Lifespan analysis of C57BL/6-hPDGFRα transgenic mice was performed using GraphPad Prism 5 software (California, USA). Survival curves, mean and median lifespan were evaluated using the Kaplan-Meier method. Survival differences between the groups were computed by the log rank test (Mantel-Cox) and by the generalized Gehan-Breslow-Wilcoxon test [63].

3.5 Quantification of mouse and human PDGFRα expression in mouse tissues

Mouse and human PDGFRα expression in mouse tissues was measured by quantitative real-time PCR. Snap-frozen skin and lungs were mechanically homogenized, using gentleMACS Dissociator (Miltenyi Biotec), in TRI Reagent (Sigma-Aldrich) and total RNA was extracted according to manufacturer's instructions. RNA (1 μg) was reverse transcribed with iScript cDNA synthesis Kit (Bio-Rad). Specific primers and probe were designed:

Mouse PDGFRα forward, 5'-GACTTCCTAAAGAGTGACCATCC-3'; Mouse PDGFRα reverse, 5'- CTTCCCAGTCCTTCAGCTTATC-3';

Mouse PDGFRα probe, 5'- ATGCGGGTGGACTCTGATAATGCG-3';

Human PDGFRα forward, 5'- ACAACCACACTCAGACAGAAG-3'; Human PDGFRα reverse, 5'-AGAATGAGCTTGAAGGCAGGCACA-3';

Human PDGFRα probe, 5'- CGTCATTCCTAGAGGTACAAAGG-3'.

Mouse and human PDGFRα-specific gBlocks DNA fragments (IDT Integrated DNA Technologies) were used to create a standard curve [64], by a 6-point serial dilution from 10^7 to 10^2 copies. gBlocks copy numbers were calculated according to the following equation [65] (#bp in gBlocks) × 617,5 g/mol/bp × (1 mol/6,02×10^{23} molecules) = weight per copy. PCR reactions were performed in triplicate for each sample, using TaqMan Fast Advanced Master Mix (Applied Biosystems) and according to the manufacturer's instructions. Cycling parameters were: 50°C for 2 minutes, 95°C for 10 minutes, then 95°C for 15 seconds and 60°C for 1 minute for 45 cycles.

3.6 Intradermal injection of human anti-PDGFRα antibodies

Twelve- to sixteen-week old heterozygous C57BL/6-hPDGFRα transgenic mice were used in this study. Only male mice were employed given the remarkable gender differences in tissue fibrosis extent and severity [66-68]. Age- and sex- matched C57BL/6 wild type (Charles River

Laboratories) mice were used as negative controls. In order to induce fibrosis, mice were injected intradermally, on days 0, 3, 6 and 9 (Figure 9A), with 2 ug of stimulatory human anti-PDGFRα monoclonal antibody (mab) VH_{PAM}-Vκ16F4 [1, 2] or with 200 ug of IgG purified from serum of patients affected by systemic sclerosis (SSc IgG), in 50 ul of phosphate buffered saline (PBS). Control animals received intradermal injection of an equal dose of non-stimulatory human anti-PDGFRα mab VH_{PAM}-Vκ13B8 [1, 2] or of IgG purified from serum of healthy controls (HC IgG). An equal volume (50 ul) of PBS was used as vehicle control. Mice were injected at each time point in four different areas (~ 1 cm^2 each) of the back skin, slightly posterior to the scapulae on both sides of the dorsal midline (Figure 9B). To minimize animal suffering, intradermal injections were performed under general anesthesia via a facial mask with a continuous flow of 1.5% isoflurane, placing the mice on heated mats to keep the rectal temperature stable at 37°C throughout the experiment [58]. Moreover, after any procedures mice were observed twice daily to monitor their health status and detect early any suffering or pathological signs. Animals were sacrificed 14 days after the first intradermal injection by isoflurane inhalation. Skin biopsies were taken in correspondence of each site of injection, and were snap frozen in liquid nitrogen and stored at -80°C for subsequent molecular analysis or were fixed in 10% Neutral Buffered Formalin Solution (Sigma-Aldrich) and embedded in paraffin. Lungs were excised, immediately washed in ice-cold PBS and were processed as previously described [58].

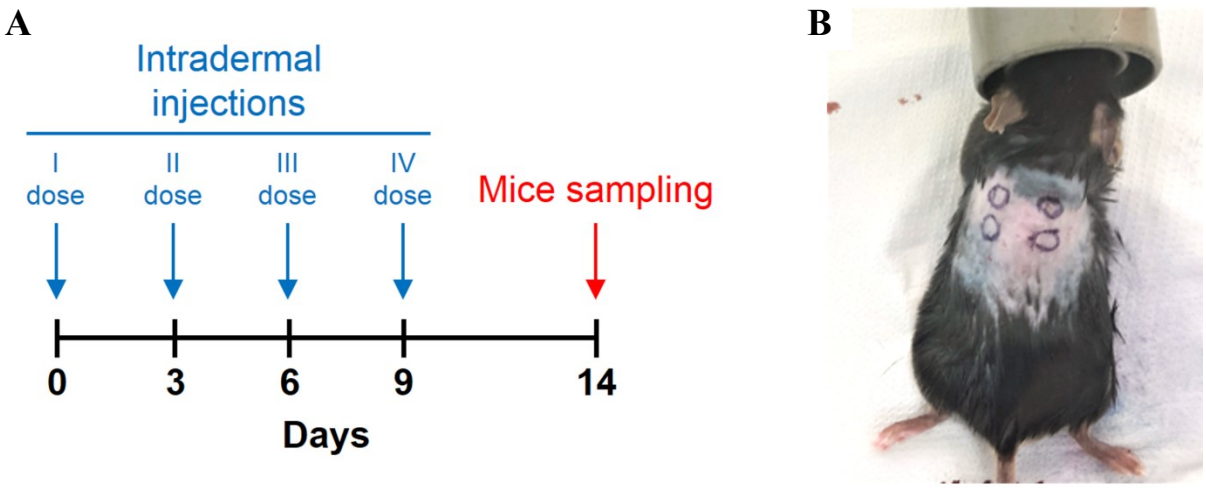

Figure 9. (**A**) Schematic of the experimental model. In order to induce skin fibrosis, mice were subjected to repeated intradermal injections, on days 0, 3, 6 and 9, and were sacrificed on day 14. (**B**) At each time point, mice were injected in four different areas (~ 1 cm^2 each) of the back skin, slightly posterior to the scapulae on both sides of the dorsal midline.

3.7 Continuous subcutaneous administration of human anti-PDGFRα antibodies

Twelve- to sixteen-week old heterozygous C57BL/6-hPDGFRα transgenic mice, male and female, were administrated human anti-PDGFRα antibodies using osmotic minipumps (ALZET 2004D; DURECT Corporation, Cupertino, CA) [3] containing either 200 µl PBS as vehicle control or SSc-MabVH_{PAM}-Vκ16F4 (100 µg) or SSc-MabVH_{PAM}-Vλ16F4 (100 µg) or SSc-Mabs VH_{PAM}-Vκ16F4+ VH_{PAM}-Vλ16F4 (50 µg + 50 µg) for 28 days (Figure 10A).

On day 0, osmotic minipumps were implanted under the back skin of mice slightly posterior to the scapulae (Figure 10B). To minimize animal suffering, minipumps implantation were performed under general anesthesia via a facial mask with a continuous flow of 1.5% isoflurane, placing the mice on heated mats to keep the rectal temperature stable at 37°C throughout the experiment [58]. Moreover, after any procedures mice were observed twice daily to monitor their health status and detect early any suffering or pathological signs.

Pumps were removed on day 28. Lung and skin tissues were harvested for histological and gene expression analysis and hydroxyproline assay. Skin samples were obtained from the dorsal area, approximately 2 cm posterior to the pump implantation site, and abdominal area.

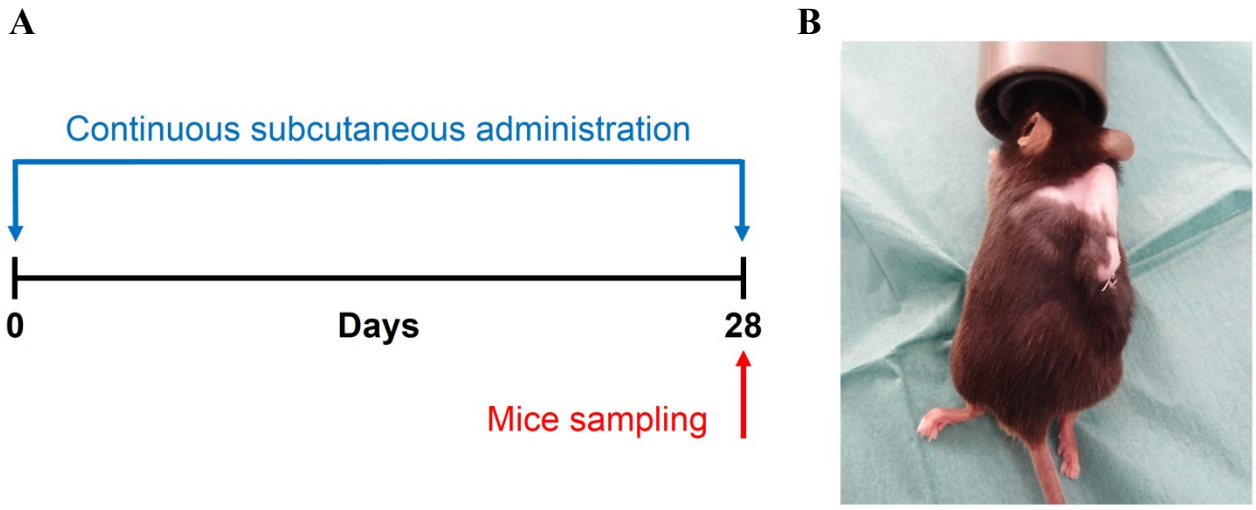

Figure 10. (**A**) Schematic of the experimental model. In order to induce systemic fibrosis, mice were subjected to continuous subcutaneous administration of human anti-PDGFRα antibodies or PBS for 28 days and were sacrificed on day 28. (**B**) Minipump was implanted subcutaneously in the back skin area, slightly posterior to the scapulae.

3.8 Histology and Immunohistochemistry

Paraffin-embedded skin and lung tissues blocks were serially cut into 5 μm thick sections and processed as described [69]. Serial skin sections were stained with hematoxylin and eosin (H&E) (Bio-Optica, Milano, Italy) and with Picrosirius Red or Masson's Trichrome. Serial lung sections were stained with hematoxylin and eosin (H&E) and Masson's Trichrome. For immunohistochemistry, antigen retrieval was performed with a pressure cooker (90°C, 20 minutes), soaking the sections in 0.01 M sodium citrate buffer pH 6.0. After a rinse in PBS, sections were treated with 3% H_2O_2 in H_2O at room temperature for 10 minutes to block endogenous peroxidase activity, rinsed with PBS and incubated with 5% Normal Serum (Vector Laboratories) in a humidified chamber at room temperature for 25 minutes.

Mouse macrophages were stained with Mouse Anti-Mouse Arginase I Monoclonal Antibody (1:200, sc-271430, Santa Cruz Biotechnology) in a humidified chamber at 4°C overnight.

After PBS rinse, sections were incubated with Biotinylated Horse Anti-Mouse IgG Antibody (1:200; Vector Laboratories) in a humidified chamber at room temperature for 30 minutes. Immunoreactivity was developed using VECTASTAIN ABC Peroxidase Kit (Vector Laboratories) and SIGMA FAST 3,3′-Diaminobenzidine Tablets (Sigma-Aldrich). Sections were counterstained with haematoxylin, dehydrated and mounted with Eukitt Quick-Hardening Mounting Medium (Sigma-Aldrich).

Skin and Lung sections were observed under a Nikon Eclipse E800 light microscope and digital images were captured with a Nikon DXM 1220 camera. In each section, Picrosirius Red and Masson's Trichrome positive area was measured in five randomly chosen fields using the ImageJ software (http://rsbweb.nih.gov/ij). Dermal thickness was calculated at 10× microscopic magnification by measuring the distance (μm) between the epidermal-dermal junction and the dermal-subcutaneous fat junction in five randomly selected fields for each H&E skin section [54]. Measurement was performed by two independent observers in blind fashion. The average positive stained area per sample was expressed as a percentage of the observed area in sterile saline-treated control mice and used for statistical analysis.

Immunoreactive cells were counted in five randomly chosen high-power fields per section with Nikon LUCIA IMAGE software (version 4.61; Laboratory Imaging, Praha, Czech Republic). Cell count was performed by two independent observers in blind fashion. The average positive stained cell number per sample was used for statistical analysis.

3.9 Determination of Collagen in Mouse Skin and Lung

Skin and lung samples were homogenized in TRI Reagent (Sigma-Aldrich) and total RNA was extracted according to manufacturer's instructions. RNA was further processed as described [1]. Specific primers for mouse genes were:

Col1A1 forward, 5'-ACATGTTCACGTTTGTGGACC-3'; Col1A1 reverse: 5'-TAGGCCATTGTGTATGCAGC-3'.

Cyclophilin forward, 5'-GTGTTCTTCGACATCACGGC-3'; Cyclophilin reverse, 5'-GTGTT CTTCGACATCACGGC-3';

18S rRNA forward, 5'-AGTCCCTGCCCTTTGTACACA-3'; 18S rRNA reverse, 5'-CGATCCGAGGGCCTCACTA-3';

Human/Mouse GAPDH forward, 5'-CAGCGACACCCACTCCTCCAC CTT-3'; Human/Mouse GAPDH reverse, 5'-CATGAGGTCCACCACCCTG TTGCT-3';

Reactions were performed in triplicate for each sample, in a volume of 25 µl containing 50 nanograms of cDNA, 12,5 µl iQ SYBR Green Supermix (Bio-Rad) and 400 nM of primers. Cycling parameters were: denaturation at 95°C for 15 seconds and annealing at 60°C for 1 minute, for 40 cycles. After normalizing data to GAPDH, cyclophilin and 18S rRNA, gene expression relative to PBS-treated control mice was calculated by the ΔΔCt method.

3.10 Hydroxyproline Assay

To quantify the amount of collagen in mouse lung specimens, hydroxyproline content was measured by Hydroxyproline Assay Kit (Sigma-Aldrich, #MAK008), according to the manufacturer's instructions. Absorbance at 560 nm was determined with a microplate reader (Elisa Plate Reader, Tecan) and values were converted to hydroxyproline content using a standard curve. The collagen amount (µg) was expressed relative to PBS-treated control mice.

3.11 Protein isolation and Western blotting

Snap-frozen skin and lung biopsies were placed in an appropriate volume (10 mg tissue/100 µl lysis buffer) of RIPA lysis buffer supplemented with Protease and Phosphatase Inhibitors Cocktail (Cell Signaling Technology) and mechanically homogenized using gentleMACS Dissociator (Miltenyi Biotec). Protein concentration of skin and homogenates were measured by Bradford Assay (Bio-Rad). 30 ug of total proteins were loaded onto 4-12% Bolt Bis-Tris Plus

polyacrylamide gels (ThermoFisher Scientific), transferred onto nitrocellulose membrane and blocked for 2 hours in TBS + 0,5% Tween-20 (TBS-T) containing 5% Blotto Non-Fat Dry Milk (Santa Cruz Biotechnology). Mouse anti-human PDGFRα (R&D Systems, #mab322, 1ug/ml) and mouse anti-human actin (Santa Cruz Biotechnology, #sc-8432) primary antibodies were then added to membranes and incubated at 4 °C overnight. Blots were washed with TBS + 0.5% Tween-20 and a goat anti-mouse IgG-HRP (Santa Cruz Biotechnology, #sc-2005) secondary antibody was added for 1 hour. Blots were finally imaged using ChemiDoc™ Imaging System (Bio-Rad). Quantification of protein signals was measured by densitometry using Quantity One Basic software (Bio-Rad).

3.12 Statistical Analysis

All quantitative data were expressed as mean ± SEM. Data were analyzed using Mann-Whitney test for nonparametric values, unpaired and two-tailed Student t test for parametric values and one-way ANOVA to compare more than two groups. All statistical analyses were performed using GraphPad Prism 5 software (California, USA). P values < 0.05 were considered significant.

4 RESULTS

4.1 Alignment of human and mouse PDGFRα

Human and mouse PDGFRα alignment of critical motif components of discontinuous epitope revealed crucial single point mutations between amino acid stretches (Figure 11).

Figure 11. Amino acid alignment of human and mouse PDGFRα extracellular domain.

4.2 Generation of a human PDGFRα-transgenic mouse

We designed a knock-in vector that specifically drives the ubiquitous expression of human PDGFRα cDNA, under control of the strong CAG promoter, into the Rosa26 locus on mouse chromosome 6, while simultaneously not affecting the expression of the endogenous receptor. An IRES-GFP reporter gene was cloned downstream of the human PDGFRα sequence to detect transgene expression.

C57BL/6 ES cells were used for gene targeting. Correctly targeted ES clones were confirmed by Southern Blotting, then selected for blastocyst microinjection, followed by chimera production. Founders were confirmed as germline transmitted via crossbreeding with Cre deleter. In the end, one male and two female F2 heterozygous C57BL/6-hPDGFRα mice were obtained and crossbreed to establish the new transgenic colony.

4.3 Characterization of human PDGFRα-transgenic mice

Both newborn and adult transgenic mice were daily monitored to early detect any suffering or distress symptoms. Moreover, mouse cohorts were observed over time to evaluate animal viability and welfare. C57BL/6-hPDGFRα transgenic mice were healthy, fertile, and did not display any apparent developmental abnormalities or pathological features.

All animals grew to the normal size and weight, and did not reveal any change in morphology when compared with C57BL/6 wild type mice [40].

Survival curves of C57BL/6-hPDGFRα transgenic mice (Figure 12A) were comparable to those obtained from C57BL/6 wild type mice (data not shown), with no significant reduction of median survival (Figure 12B) [62, 70].

However, lifespan analysis of C57BL/6-hPDGFRα transgenic mice showed a significant difference (log rank test, P = 0,0118; Wilcoxon test, P = 0,0276) in survival curves between genders, with a mean and a median lifespan of 110,8 and 110 weeks in males (n = 35) and of 100,1 and 97 weeks (n = 12) in females, respectively.

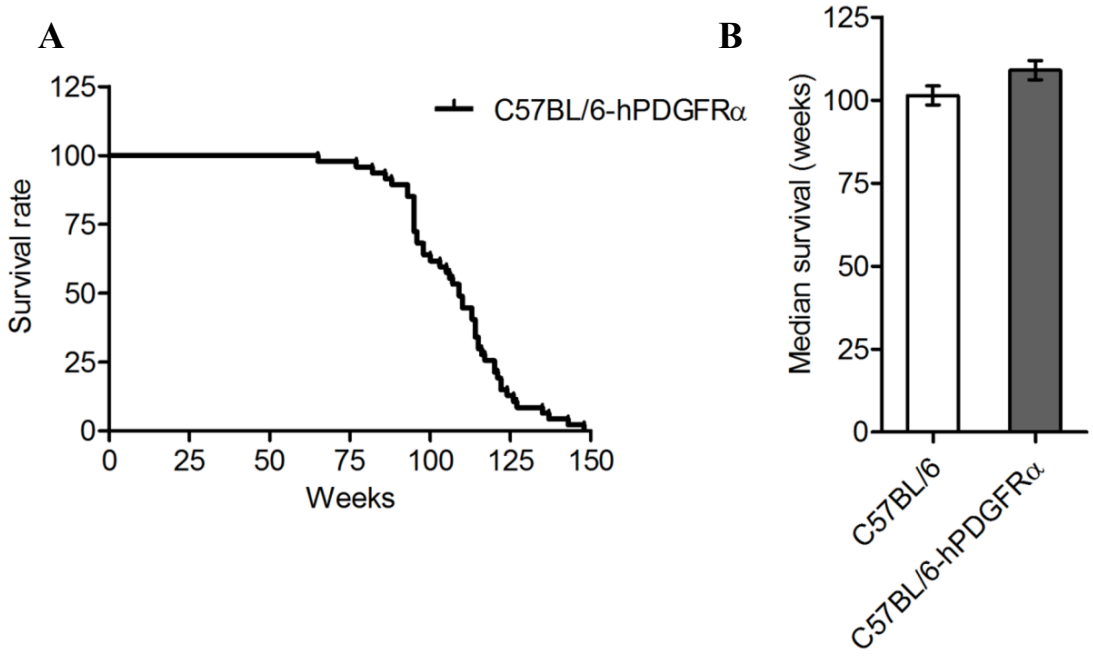

Figure 12. (A) Kaplan-Meier survival curve for C57BL/6-hPDGFRα transgenic mice. The cumulative survival rate was plotted against age measured in weeks. **(B)** Comparison between median survival in C57BL/6-hPDGFRα transgenic mice(109 weeks) and C57BL/6-wild type mice (101,4 weeks).

4.4 Human PDGFRα transgene transmission and tissue expression

PCR genotyping of the mouse offspring was performed to assess genetic transmission of the transgene to the progeny. Human PDGFRα transgene was stably inherited through the different mouse generations, with a transmission rate to the progeny of approximately 50%.

Moreover, in order to confirm the effective expression of the transgene in mouse tissues, copy number of human PDGFRα transcript in mRNA extracted from skin and lung biopsies of C57BL/6-hPDGFRα transgenic mice was evaluated by quantitative real-time PCR.

Our data demonstrated similar expression levels of human PDGFRα in all mouse skin and lung tissues (Figure 13A), with a maximum log-linear detection range of one order of magnitude in the standard curve (Figure 13B), from 10^3 to 10^4 copies/ul cDNA per sample [64].

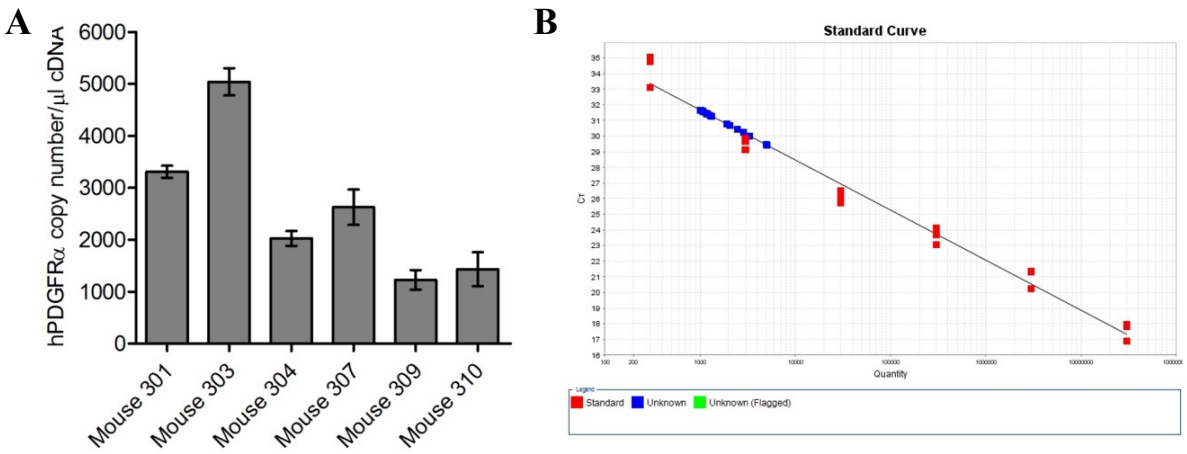

Figure 13. (**A**) Human PDGFRα transgene expression by qPCR in mRNA extracted from skin biopsies of C57BL/6-hPDGFRα transgenic mice. Similar transgene copy numbers were detected, with a maximum log-linear range of one order of magnitude in the standard curve (**B**). Comparable data was obtained in lung tissue.

In parallel, Western blot analysis of skin and lung lysates obtained from C57BL/6-hPDGFRα transgenic mice showed similar protein levels of human PDGFRα in all tested samples (Figure 14). Protein integrity was also confirmed.

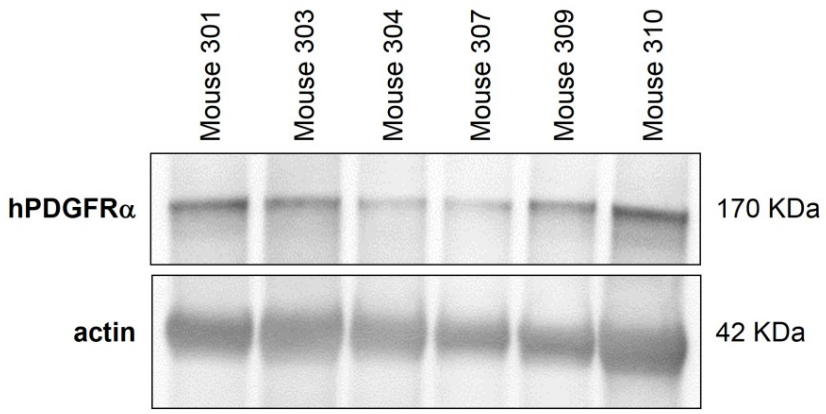

Figure 14. Human PDGFRα protein levels in whole skin tissue lysates obtained from C57BL/6-hPDGFRα transgenic mice. Comparable data was obtained in lung tissue.

4.5 Induction of skin fibrosis by intradermal injection of human anti-PDGFRα antibodies

Intradermal injection, at days 0, 3, 6 and 9, of stimulatory human anti-PDGFRα mab VH_{PAM}-V_{κ}16F4 or SSc IgG into the back skin of C57BL/6-hPDGFRα transgenic mice (n = 8/group) resulted in significant skin fibrosis. Histological analysis of skin tissues sampled at day 14 documented, in fact, in comparison with PBS, a marked dermal thickening (Figure 15A, Figure 16) with increased deposition of densely packed and irregularly arranged collagen bundles (Figure 16A). Moreover, the glandular and subcutaneous adipose tissue layers were reduced and partially replaced by infiltrating collagen fibers [3, 71]. Conversely intradermal injection of both non-stimulatory human anti-PDGFRα mab VH_{PAM}-V_{κ}13B8 and N IgG did not cause any skin change. Interestingly, all C57BL/6 wild type-treated mice (n = 8/ group) demonstrated normal skin histology (Figure 15B, Figure 17B). To determine if augmented collagen deposition was due to enhanced collagen synthesis, Col1A1 gene expression was analyzed by quantitative real-time PCR in mRNA extracted from skin. We observed a significant increase in Col1A1 mRNA expression following intradermal injection of stimulatory human anti-PDGFRα mab VH_{PAM}-V_{κ}16F4 or SSc IgG into the back skin of C57BL/6-hPDGFRα transgenic mice. In contrast, intradermal injection of non-stimulatory mab VH_{PAM}-V_{κ}13B8 or N IgG did not up-regulate collagen transcription. Moreover, all C57BL/6 wild type-treated mice showed basal Col1A1 gene expression levels (Figure 18).

A

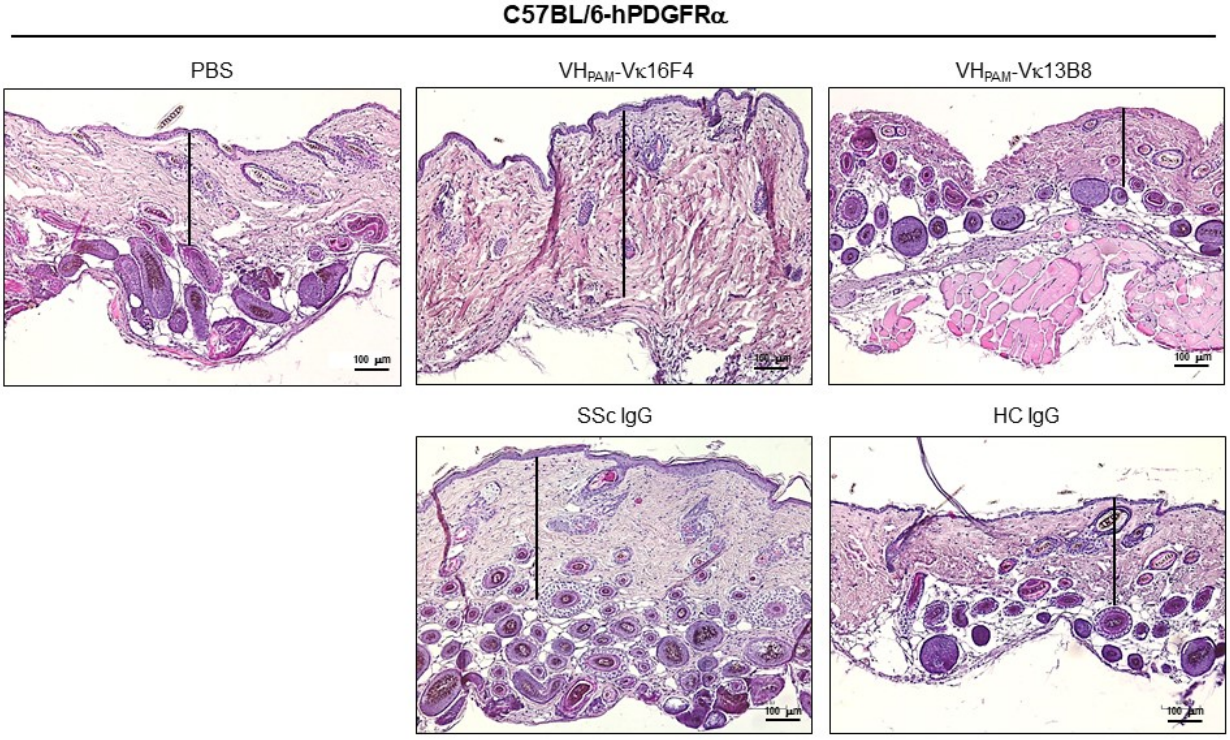

B

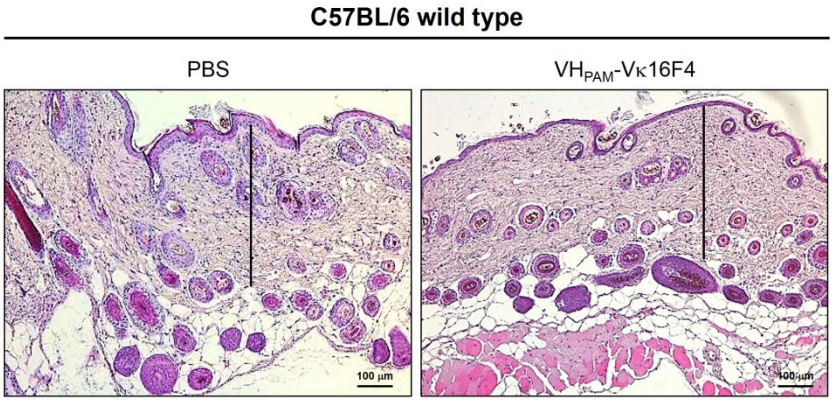

Figure 15. (A) Skin sections obtained at day 14 from C57BL/6-hPDGFRα transgenic mice (n=8 per group) were stained with H&E. Intradermal injection of stimulatory human SSc-MabVH_{PAM}-Vκ16F4 or SSc-IgG resulted in dermal thickening, where as non-stimulatory humanSSc-MabVH_{PAM}-Vκ13B8 or HC-IgG did not induce any significant skin tissue alterations compared to vehicle control (PBS).
(B) Skin sections obtained at day 14 from C57BL/6 wild type mice (n=8 per group) were stained with H&E. Intradermal injection of stimulatory human SSc-Mab VH_{PAM}-Vκ16F4 did not induce any significant dermal thickness, compared to vehicle control (PBS). Representative microscopic images (10×magnification) of three independent experiments are shown.

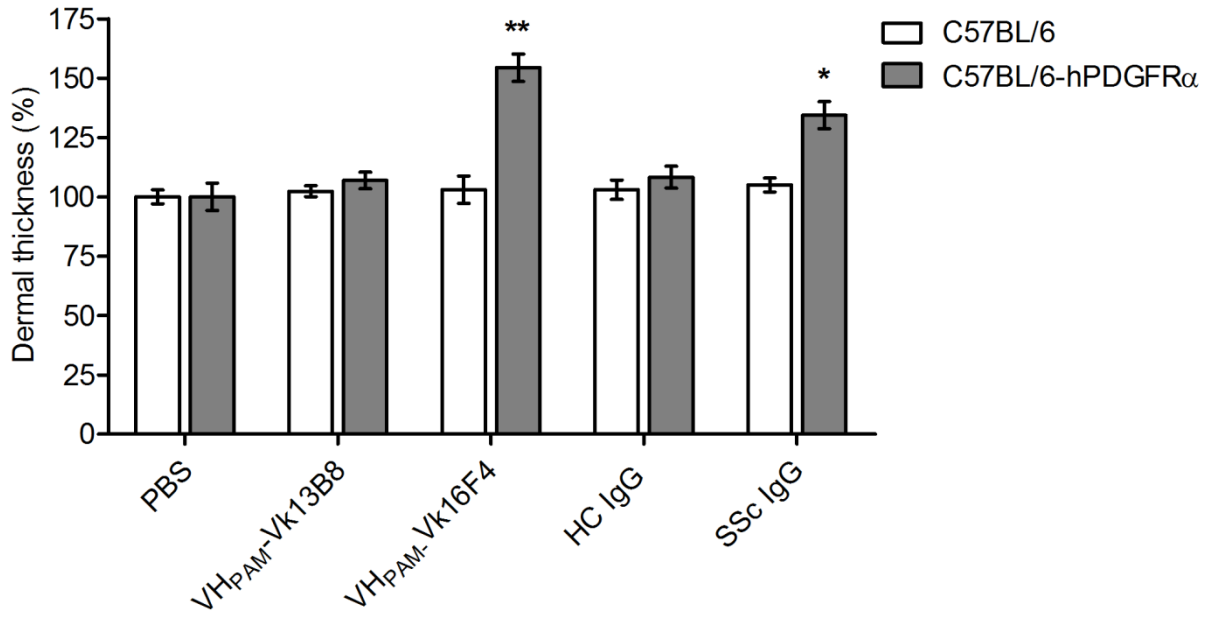

Figure 16. Dermal thickness of skin sections obtained at day 14 from C57BL/6-hPDGFRα transgenic and C57BL/6 wild type mice (n=8 per group) that received the aforementioned treatments. Dermal thickness was calculated at 10x microscopic magnification by measuring the distance (μm) between the epidermal-dermal junction and the dermal-subcutaneous fat junction in five randomly selected fields for each skin section.

A

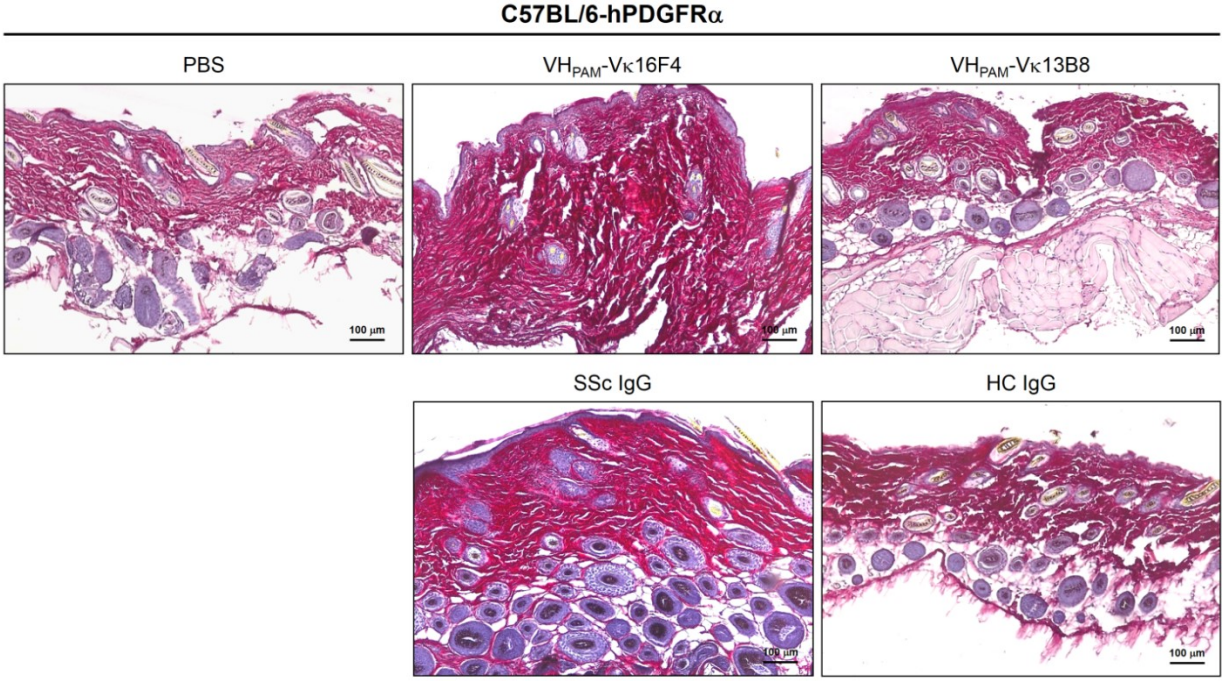

B

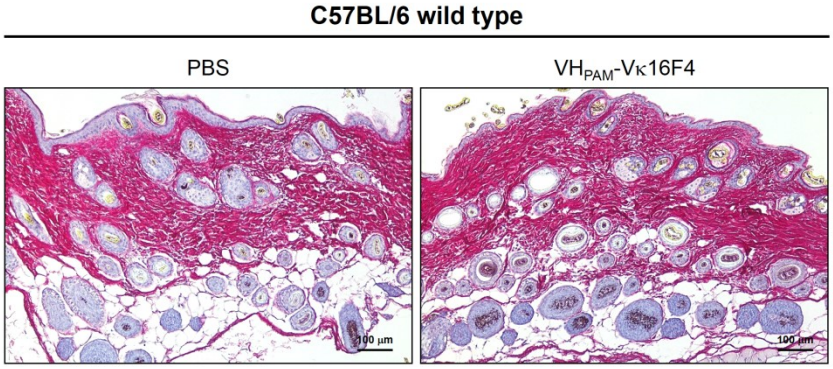

Figure 17. (A) Picrosirius Red staining of skin sections obtained at day 14 from C57BL/6-hPDGFRα transgenic mice (n=8 per group). Intradermal injection of stimulatory human SSc-MabVH$_{PAM}$-Vκ16F4 or SSc-IgG resulted in dermal thickening and increased collagen deposition, where as non-stimulatory human SSc-MabVH$_{PAM}$-Vκ13B8 or HC-IgG did not induce any significant skin tissue alterations compared to vehicle control (PBS). **(B)** Picrosirius Red staining of skin sections obtained at day 14 from C57BL/6 wild type mice (n=8 per group). Intradermal injection of stimulatory human SSc-Mab VH$_{PAM}$-Vκ16F4 did not induce any significant skin tissue changes compared to vehicle control (PBS). Representative microscopic images (10×magnification) of three independent experiments are shown.

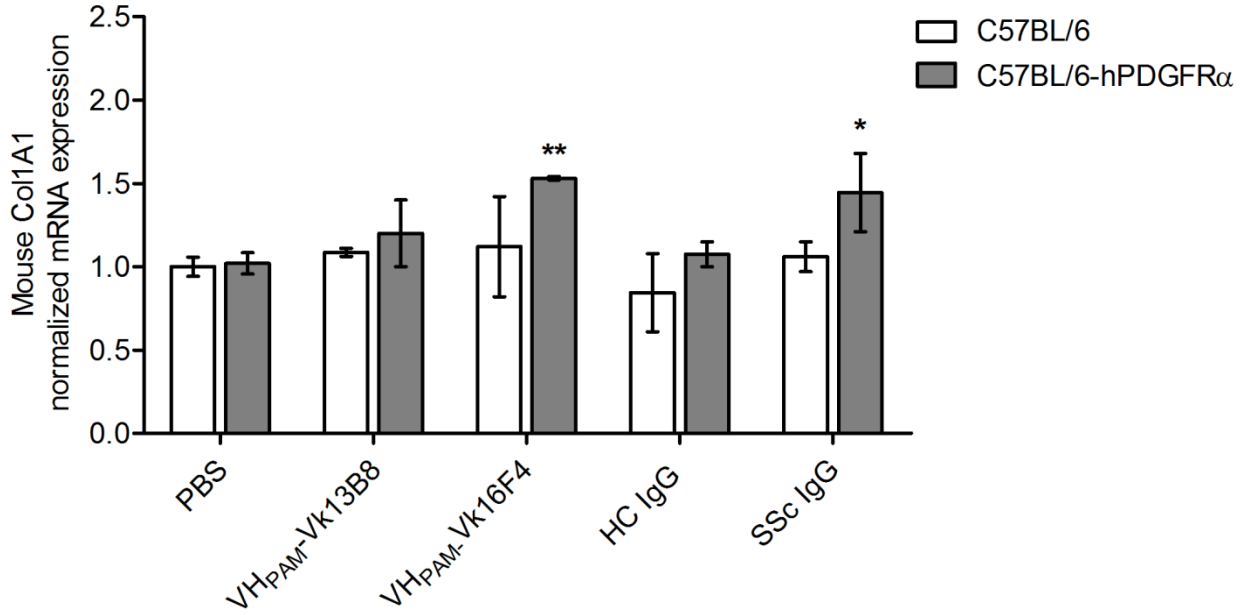

Figure 18. Gene expression analysis of mouse Col1A1 in skin mRNA obtained at day 14 from C57BL/6 hPDGFRα transgenic and C57BL/6 wild type mice (n=8 per group) that received the aforementioned treatments. Results are mean ±SD (n=8 per group) expressed as a percent of the value obtained from PBS-treated mice and are representative of three independent experiments. *= P<0.05,**= P<0.01 compared to PBS-treated mice.

4.6 Induction of skin and lung fibrosis by continuous subcutaneous administration of human anti-PDGFRα antibodies

Continuous subcutaneous administration, using an osmotic pump, from day 0 to day 28 of stimulatory human anti-PDGFRα SSc-MabVH_{PAM}-Vκ16F4 or SSc-MabVH_{PAM}-Vλ16F4 or SSc-MabVH_{PAM}-Vκ16F4+ VH_{PAM}-Vλ16F4 in the back skin area of C57BL/6-hPDGFRα transgenic mice (n = 8/group) resulted in a relevant skin fibrosis and initial lung damage.

Histological analysis of skin sampled at day 28 documented, in fact, in comparison with PBS, a dermal thickening with increased deposition of densely packed and irregularly arranged collagen bundles (Figure 19, Figure 20). Moreover, the glandular and subcutaneous adipose tissue layers were reduced and partially replaced by infiltrating collagen fibers [3, 71]. Conversely continuous subcutaneous administration of vehicle control (PBS) did not cause any skin changes.

To determine if augmented collagen deposition was due to enhanced collagen synthesis, Col1A1 gene expression was analyzed by quantitative real-time PCR in mRNA extracted from skin. We observed an increase in Col1A1 mRNA expression following continuous subcutaneous infusion of human anti-PDGFRα SSc-MabVH_{PAM}-Vκ16F4 or SSc-MabVH_{PAM}-Vλ16F4 or SSc-MabVH_{PAM}-Vκ16F4+VH_{PAM}-Vλ16F4 in C57BL/6-hPDGFRα transgenic mice compared vehicle control (PBS). No significant statistically results in mice treated with VH_{PAM}-V_{κ}16F4 or SSc-MabVH_{PAM}-Vλ16F4 depend on mice variable responses (Figure 21).

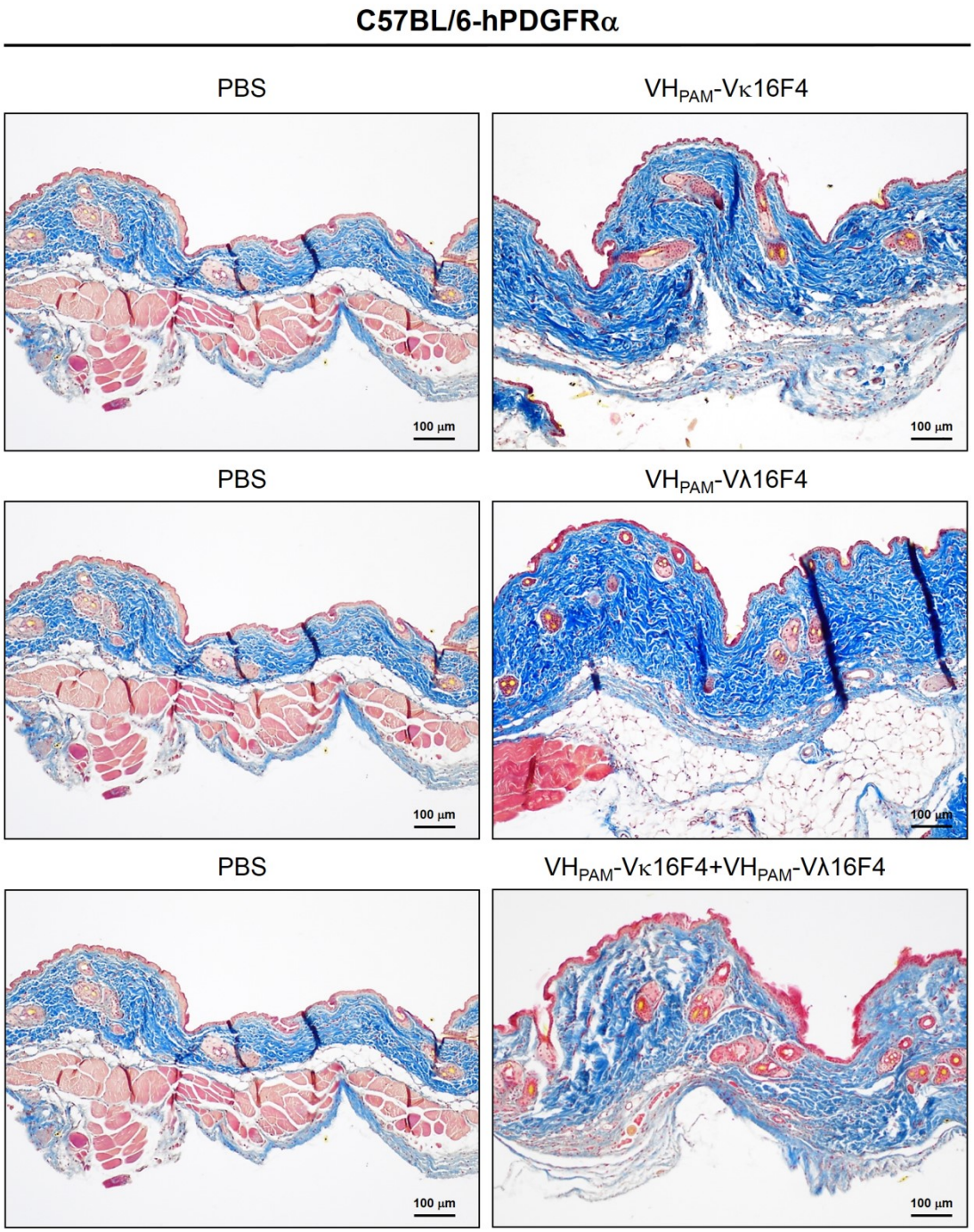

Figure 19. Masson's trichrome staining of skin sections obtained at day 28 from C57BL/6-hPDGFRα transgenic mice (n=8 per group). Continuous subcutaneous administration of SSc-MabVH$_{PAM}$-Vκ16F4 or SSc-MabVH$_{PAM}$-Vλ16F4 or SSc-Mabs VH$_{PAM}$-Vκ16F4+ VH$_{PAM}$-Vλ16F4 resulted in dermal thickening and increased collagen deposition compare to vehicle control (PBS). Representative microscopic images (10× magnification) of three independent experiments are shown.

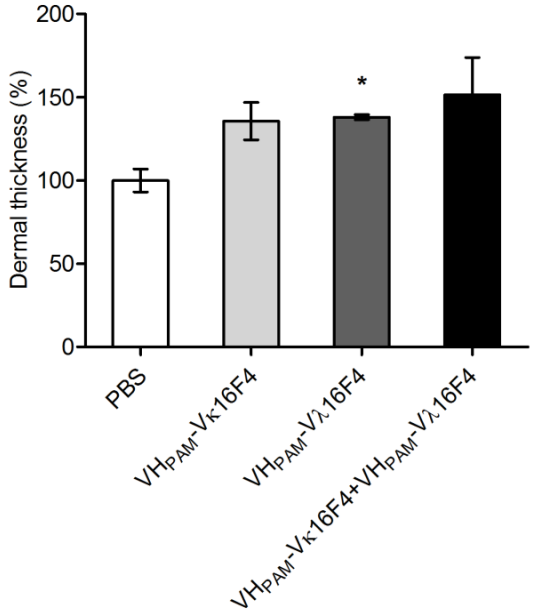

Figure 20. Dermal thickness of skin sections obtained at day 28 from C57BL/6-hPDGFRα transgenic (n=8 per group) that received the aforementioned treatments. Dermal thickness was calculated at 10x microscopic magnification by measuring the distance (μm) between the epidermal-dermal junction and the dermal-subcutaneous fat junction in five randomly selected fields for each skin section.

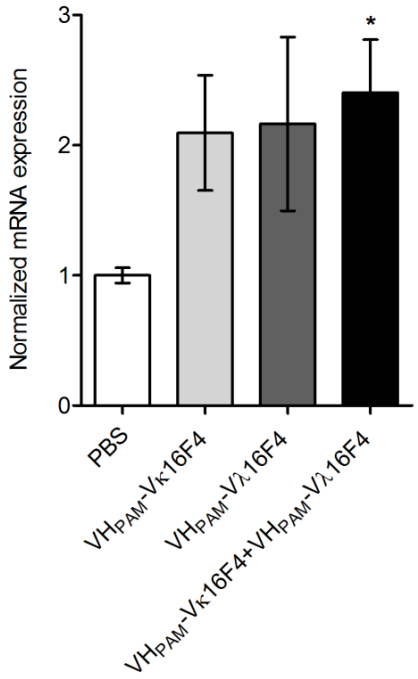

Figure 21. Gene expression analysis of mouse Col1A1 in skin mRNA obtained at day 28 from C57BL/6 hPDGFRα transgenic that received the aforementioned treatments. Results are mean ±SD (n=8 per group) expressed as a percent of the value obtained from PBS-treated mice and are representative of three independent experiments.
*= P<0.05,**= P<0.01 compared to PBS-treated mice.

Histological analysis of lung sampled at day 28 documented, in comparison with PBS, an initial damage with perivascular and peribronchiolar increased collagen deposition in C57BL/6-hPDGFRα treated with SSc-MabVH_{PAM}-Vκ16F4 or SSc-MabVH_{PAM}-Vλ16F4 (Figure 22A). Moreover, continuous subcutaneous administration of SSc-MabVH_{PAM}-Vκ16F4+VH_{PAM}-Vλ16F4 induced prominent lung inflammation, with a diffuse alveolar and interstitial inflammatory cell infiltration, accompanied by bronchoalveolar hyperplasia and distortion of the

normal architecture of the alveoli. PBS treated control mice (n. = 8) demonstrated normal lung histology.

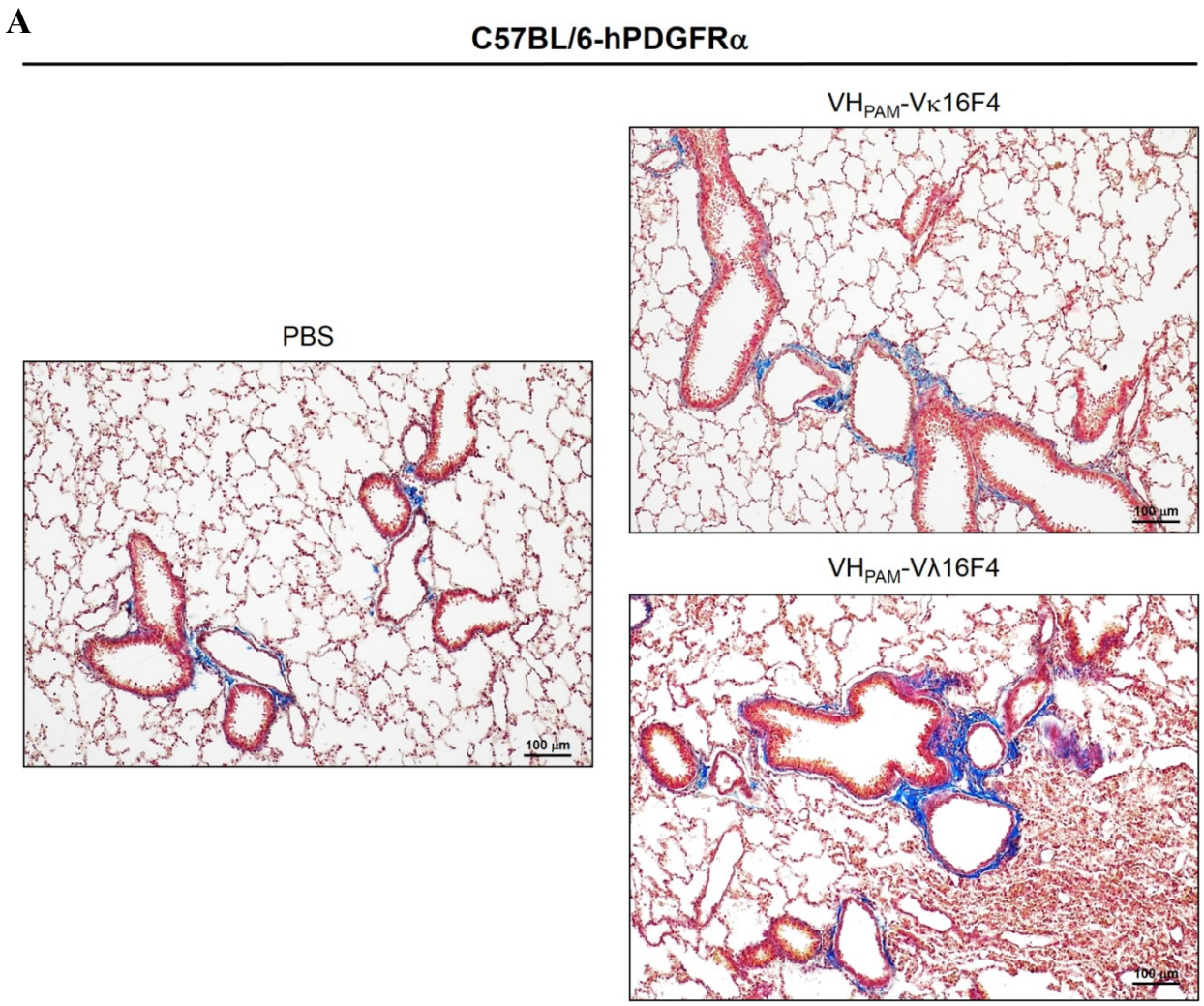

Figure 22. **(A)** Masson's trichrome staining of lung sections obtained at day 28 from C57BL/6-hPDGFRα transgenic mice (n=8 per group). Continuous subcutaneous administration of SSc-MabVH$_{PAM}$-Vκ16F4 or SSc-MabVH$_{PAM}$-Vλ16F4 resulted in perivascular and peribronchiolar increased collagen deposition compare to normal lung architecture in vehicle control (PBS). Representative microscopic images (10× magnification) of three independent experiments are shown.

Inflammatory cell infiltration were characterized by H&E and by immunohistochemistry for Arginase I, a specific marker of M2 macrophages. We could observe a significant increase of arginase-1 positively stained cells count in the alveoli and interstitial spaces compared to PBS-treated control (Figure 22 B, Figure 23).

B

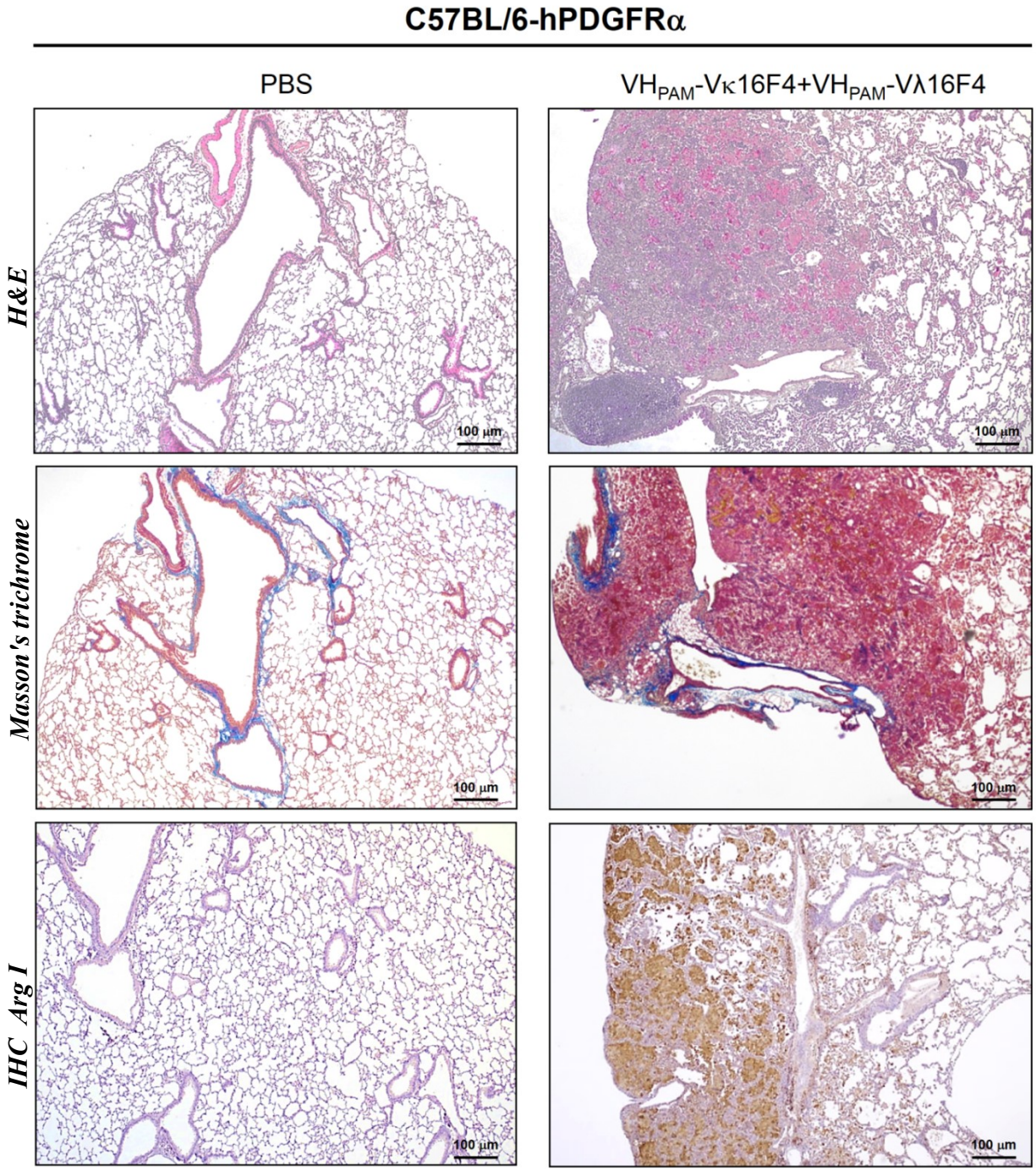

Figure 22. **(B)** Massive inflammatory infiltrates were observed by H&E in lung sections obtained at day 28 from C57BL/6-hPDGFRα transgenic mice treated with continuous subcutaneous administration of SSc-MabVH_{PAM}-Vκ16F4+VH_{PAM}-Vλ16F4 compare to vehicle control (PBS). Masson's trichrome staining demonstrated increased perivascular and peribronchiolar deposition of collagen content. Inflammatory cell infiltration were characterized by immunohistochemistry for arginase I. Increase of M2 macrophages positive cells were observed in mice stimulated by SSc-MabsVH_{PAM}-Vκ16F4+VH_{PAM}-Vλ16F4. Representative microscopic images (4× magnification) of three independent experiments are shown.

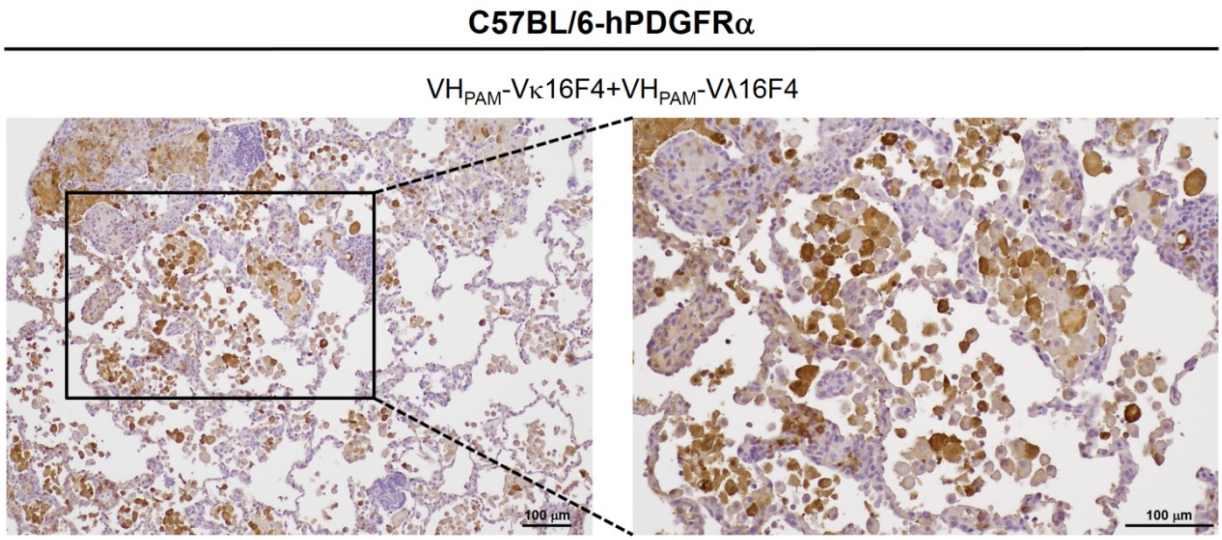

Figure 23. Arginase-I positive cells in lung sections obtained at day 28 from C57BL/6-hPDGFRα transgenic mice (n=8 per group) after continuous subcutaneous administration of SSc-MabsVH$_{PAM}$-Vκ16F4+VH$_{PAM}$-Vλ16F4 that exhibit, at higher magnification, an alveolar distribution. Lung sections obtained were immunostained with anti-Arginase I antibody. Representative microscopic images (10× and 20× magnification) of three independent experiments are shown.

Col1A1 gene expression, analyzed by quantitative real-time PCR in mRNA extracted from lung tissue, revealed an increase in Col1A1 mRNA expression following continuous subcutaneous infusion of human anti-PDGFRα SSc-MabVH$_{PAM}$-Vκ16F4 or SSc-MabVH$_{PAM}$-Vλ16F4 or SSc-MabVH$_{PAM}$-Vκ16F4+ VH$_{PAM}$-Vλ16F4 in C57BL/6-hPDGFRα transgenic mice compared to vehicle control (PBS). No statistically significant results in mice treated with SSc-MabVH$_{PAM}$-V$_{κ}$16F4 or SSc-Mabs VH$_{PAM}$-Vκ16F4+VH$_{PAM}$-Vλ16F4 depend on mice variable responses (Figure 24 A).

To better assess fibrosis in C57BL/6-hPDGFRα mice treated with human anti-PDGFRα antibodies, quantification of total soluble and insoluble lung collagen content was performed using the gold standard hydroxyproline assay [72], which confirmed a significant increase in collagen content in the lungs of human anti-PDGFRα antibodies -treated mice, compared to mice that received PBS. No statistically significant results in mice treated with SSc-MabVH$_{PAM}$-Vκ16F4 depend on mice variable responses (Figure 24 B).

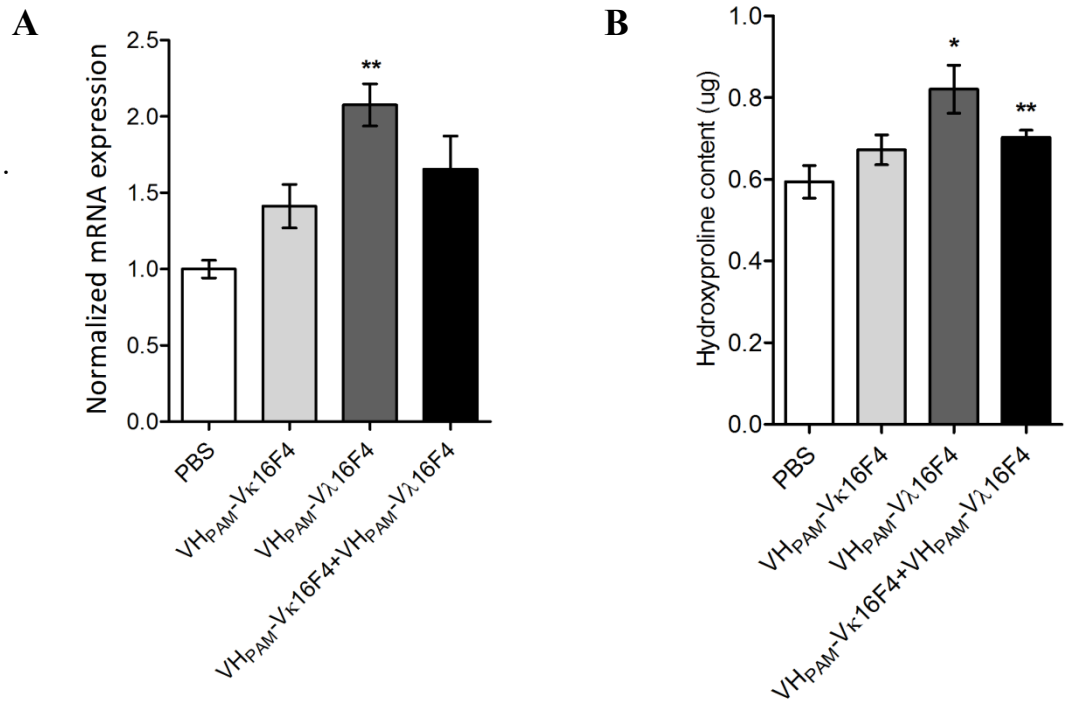

Figure 24. (A) Gene expression analysis of mouse Col1A1 in lung mRNA obtained at day 28 from C57BL/6 hPDGFRα transgenic mice that received the aforementioned treatments. Results are mean ±SD (n=8 per group) expressed as a percent of the value obtained from human anti-PDGFRα antibodies -treated mice and are representative of three independent experiments.
*= P<0.05,**= P<0.01 compared to PBS-treated mice
(B) Hydroxyproline content in lung tissue of C57BL/6 hPDGFRα transgenic mice that received the aforementioned treatments.
Results are mean ± SD (n = 8 per group) expressed as a percent of the value obtained from human anti-PDGFRα antibodies-treated mice and are representative of three independent experiments. *= P < 0.05, ** = P < 0.01 compared to PBS treated mice.

Enhanced perivascular collagen deposition in C57BL/6-hPDGFRα transgenic mice treated with human anti-PDGFRα antibodies was accompanied by increased expression of α-SMA, a marker of fibroblasts with collagen-secreting phenotype. Increased positive staining of vascular smooth muscle cells surrounding the endothelial layer was more evident in small vessels (Figure 25).

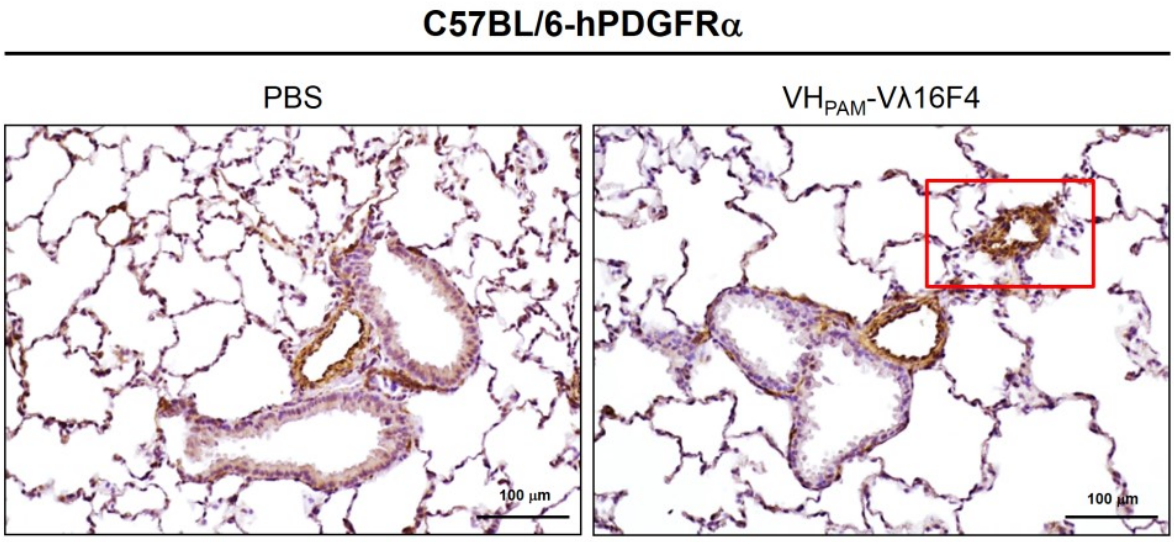

Figure 25. Immunohistochemical determination of α-SMA in lung tissue**.** Increased perivascular deposition of α-SMA in lungs sections obtained at day 28 from C57BL/6-hPDGFRα transgenic mice (n=8 per group) after continuous subcutaneous administration of SSc-MabVH_{PAM}-Vλ16F4 (representative image, similar results were obtained using SSc-MabVH_{PAM}-Vκ16F4 or SSc-Mabs VH_{PAM}-Vκ16F4+ VH_{PAM}-Vλ16F4) compare to vehicle control (PBS). Lung sections were immunostained with anti α-SMA antibody. Representative microscopic images (20× magnification) of three independent experiments are shown.

4 DISCUSSION

The heterogeneous clinical manifestations of SSc represent strong challenges for the management of the patients and the understanding of pathogenesis [52].
The availability of animal models replicating the hallmarks of the human disease would be essential for solving the complexity of this disease.
Although several animal models recapitulating some SSc aspects have been reported, the development of novel models continues to be vitally important in order to provide new insights in the pathogenesis of SSc, to identify new biomarkers of disease activity and drug response.

In a previous study, Prof. Armando Gabrielli's research group was able to generate monoclonal autoantibodies (mAb) using immunoglobulin sequences obtained from the peripheral blood mononuclear cells of SSc patients, that were specific for PDGFRα and able to reproduce in vitro the agonistic effects of total IgG purified from serum of SSc patients [1].
These autoantibodies, unlike others previously described in literature, possess biological activity and can contribute, as pathogenic factors, to tissue and vascular damage in SSc. In particular, by targeting PDGFRα on cell surface of fibroblasts and smooth muscle cells , these stimulatory autoantibodies have the ability to induce a profibrotic profile characterized by excessive proliferation and increased collagen gene transcription.

Based on this evidence, to definitively prove that PDGFRα activation is a relevant pathway in the development of SSc fibrosis we generated a novel humanized mouse model characterized by concomitant expression of human and mouse PDGF receptor α, herein called C57BL/6-hPDGFRα.
This strategy was decided in order to avoid disruption of physiological murine PDGF-PDGFRα signaling pathway, and provide a specific target for agonistic autoantibodies, a scenario ideally resembling what should be occurring in human subjects during the development of SSc disease.
Notably, human PDGFRα compared to mouse counterpart carries several aminoacid mutations in the epitope of agonistic autoantibodies.
Our prediction that agonistic SSc-Mabs would not bind and stimulate mouse PDGFRα was indeed confirmed by experiments with wild-type mice.

C57BL/6-hPDGFRα is the first PDGFRα humanized mouse ever generated; the characterization of this model showed an healthy phenotype with no side effects.
Unlike the humanized-skin-SCID model previously used to test the biological activity of SSc Mabs, C57BL/6-hPDGFRα mice are immunocompetent, again a scenario similar to human subjects affected by SSc [2].
The expression of hPDGFRα transgene was stable and ubiquitous, both at gene and protein levels; all mice grew to the normal size and weight, and did not reveal any change in morphology or natural physiology when compared with C57BL/6 wild type mice.

Two different administration routes of Mabs were chosen:

i. intradermal injection
ii. subcutaneous administration

i. Intradermal injection of human anti-PDGFRα antibodies in C57BL/6-hPDGFRα mice resulted in significant skin fibrosis, consisting of marked dermal thickness and increased deposition of collagen bundles.

Specifically, this phenotype was induced by injection of stimulatory SSc-MabVH_{PAM}-Vκ16F4 or SSc-IgG, whereas non-stimulatory human SSc-Mab VH_{PAM}-Vκ13B8 or HD-IgG did not induce any significant skin tissue alterations compared to vehicle control.
Remarkably, as anticipated above, C57BL/6 wild type mice did not show any significant skin tissue changes with any antibodies.

A topic of growing interest in scleroderma studies is the relationship between subcutaneous fat and dermal fibrosis. Both in SSc patients and in mouse models, dermal fibrosis is associated to thinning of the subcutaneous adipose layer [3]. This feature was confirmed also in the skin of C57BL/6-hPDGFRα mouse model in which the glandular and subcutaneous adipose tissue layers were reduced and partially replaced by infiltrating collagen fibers.

ii. Several animal models potentially useful for studying SSc pathogenesis have been described in literature. Unfortunately, no single experimental model has been described that fully reproduces the pathophysiologic spectrum of human SSc [53].

It has been reported that systemic delivery of bleomycin via continuous diffusion from subcutaneously implanted osmotic minipumps can cause fibrosis of the skin, lungs, and other internal organs [3]. Starting from this evidence, osmotic minipumps were implanted under the

back skin of C57BL/6-hPDGFRα mice and filled with anti-PDGFRα human autoantibodies in order to induce systemic fibrosis.

Our findings suggest that systemic delivery of anti-PDGFRα human autoantibodies via continuous diffusion from subcutaneously implanted osmotic minipumps could mimic SSc-like fibrosis. The amount of collagen in the skin and lung was assessed by histological methods and quantified using molecular and enzymatic techniques.

At 28 days post implantation, we observed an increased dermal collagen deposition in skin and perivascular and peribronchiolar collagen amount in lung tissues. Moreover, mice treated with a combination of SSc-Mabs VH_{PAM}-Vκ16F4 and VH_{PAM}-Vλ16F4 displayed massive inflammatory infiltrates with distortion of the normal lung architecture. In this experiment, most inflammatory cells in the alveoli and interstitial spaces were M2 macrophages, that are implicated in excessive tissue repair and subsequent organ fibrosis.

Considering that SSc is characterized by widespread peripheral microvascular injury, we focused our attention on positive staining of vascular smooth muscle cells surrounding the endothelial layer of lung microvasculature. Immunohistochemistry demonstrated increased deposition of α-SMA in small vessels of C57BL/6-hPDGFRα mice treated with SSc Mabs.

Overall, we were able to reproduce a significant skin and an initial lung fibrosis via continuous administration of stimulatory anti-PDGFRα human autoantibodies by subcutaneously implanted osmotic minipumps in C57BL/6-hPDGFRα mice. It is important to emphasize that our results are preliminary because not all of the mice undergoing treatment were responsive to this kind of stimulation.

The same extent of dermal skin fibrosis obtained by intradermal injections was replicated using osmotic minipumps implanted subcutaneously and filled with SSc Mabs.

C57BL/6-hPDGFRα mice Pump model has several advantages:

i) dermal fibrosis can be attained without laborious, repeated injections of autoantibodies

ii) may provide the opportunity to examine the effects of potential therapies on skin and lung fibrosis simultaneously.

In conclusion, intradermal injection and a well consolidated pump model are two attractive models to analyze the underlying mechanisms of fibrosis and test the efficacy of potential therapies. In particular, *in vivo* blocking of the functional epitope recognized by anti-PDGFRα autoantibodies could be a valid therapeutic strategy for inhibiting the signaling pathway involved

in SSc development. Alternatively, a decoy receptor capturing stimulatory anti-PDGFRα autoantibodies would also be an intriguing strategy, as successfully experienced in other immune-mediated disorders such as Rheumatoid Arhtritis with Etanercept molecule.

5 BIBLIOGRAFY

1. Moroncini G, Grieco A, Nacci G, Paolini C, Tonnini C, Pozniak KN, et al. Epitope Specificity Determines Pathogenicity and Detectability of Anti-Platelet-Derived Growth Factor Receptor alpha Autoantibodies in Systemic Sclerosis. Arthritis Rheumatol. 2015;67(7):1891-903. PubMed PMID: 25808833.

2. Luchetti MM, Moroncini G, Jose Escamez M, Svegliati Baroni S, Spadoni T, Grieco A, et al. Induction of Scleroderma Fibrosis in Skin-Humanized Mice by Administration of Anti-Platelet-Derived Growth Factor Receptor Agonistic Autoantibodies. Arthritis Rheumatol. 2016;68(9):2263-73. PubMed PMID: 27111463.

3. Watanabe T, Nishimoto T, Mlakar L, Heywood J, Malaab M, Hoffman S, et al. Optimization of a murine and human tissue model to recapitulate dermal and pulmonary features of systemic sclerosis. PLoS One. 2017;12(6):e0179917. PubMed PMID: 28651005.

4. Chifflot H, Fautrel B, Sordet C, Chatelus E, Sibilia J. Incidence and prevalence of systemic sclerosis: a systematic literature review. Semin Arthritis Rheum. 2008;37(4):223-35. PubMed PMID: 17692364.

5. van den Hoogen F, Khanna D, Fransen J, Johnson SR, Baron M, Tyndall A, et al. 2013 classification criteria for systemic sclerosis: an American College of Rheumatology/European League against Rheumatism collaborative initiative. Arthritis Rheum. 2013;65(11):2737-47. PubMed PMID: 24122180.

6. Denton CP, Khanna D. Systemic sclerosis. Lancet. 2017;390(10103):1685-99. PubMed PMID: 28413064.

7. Gabrielli A, Avvedimento EV, Krieg T. Scleroderma. N Engl J Med. 2009;360(19):1989-2003. PubMed PMID: 19420368.

8. Silman AJ. Epidemiology of scleroderma. Ann Rheum Dis. 1991;50 Suppl 4:846-53. PubMed PMID: 1750796.

9. Silman AJ. Scleroderma demographics and survival. J Rheumatol Suppl. 1997;48:58-61. PubMed PMID: 9150120.

10. Frech T, Khanna D, Markewitz B, Mineau G, Pimentel R, Sawitzke A. Heritability of vasculopathy, autoimmune disease, and fibrosis in systemic sclerosis: a population-based study. Arthritis Rheum. 2010;62(7):2109-16. PubMed PMID: 20506251.

11. Stern EP, Denton CP. The Pathogenesis of Systemic Sclerosis. Rheum Dis Clin North Am. 2015;41(3):367-82. PubMed PMID: 26210124.

12. Feghali-Bostwick C, Medsger TA, Jr., Wright TM. Analysis of systemic sclerosis in twins reveals low concordance for disease and high concordance for the presence of antinuclear antibodies. Arthritis Rheum. 2003;48(7):1956-63. PubMed PMID: 12847690.

13. Arnett FC, Gourh P, Shete S, Ahn CW, Honey RE, Agarwal SK, et al. Major histocompatibility complex (MHC) class II alleles, haplotypes and epitopes which confer susceptibility or protection in systemic sclerosis: analyses in 1300 Caucasian, African-American and Hispanic cases and 1000 controls. Ann Rheum Dis. 2010;69(5):822-7. PubMed PMID: 19596691.

14. Hewagama A, Richardson B. The genetics and epigenetics of autoimmune diseases. J Autoimmun. 2009;33(1):3-11. PubMed PMID: 19349147.

15. Moroncini G, Mori S, Tonnini C, Gabrielli A. Role of viral infections in the etiopathogenesis of systemic sclerosis. Clin Exp Rheumatol. 2013;31(2 Suppl 76):3-7. PubMed PMID: 23910606.

16. Manetti M, Romano E, Rosa I, Guiducci S, Bellando-Randone S, De Paulis A, et al. Endothelial-to-mesenchymal transition contributes to endothelial dysfunction and dermal fibrosis in systemic sclerosis. Ann Rheum Dis. 2017;76(5):924-34. PubMed PMID: 28062404.

17. LeRoy EC. Increased collagen synthesis by scleroderma skin fibroblasts in vitro: a possible defect in the regulation or activation of the scleroderma fibroblast. J Clin Invest. 1974;54(4):880-9. PubMed PMID: 4430718.

18. Sambo P, Baroni SS, Luchetti M, Paroncini P, Dusi S, Orlandini G, et al. Oxidative stress in scleroderma: maintenance of scleroderma fibroblast phenotype by the constitutive up-regulation of reactive oxygen species generation through the NADPH oxidase complex pathway. Arthritis Rheum. 2001;44(11):2653-64. PubMed PMID: 11710721.

19. Chizzolini C, Boin F. The role of the acquired immune response in systemic sclerosis. Semin Immunopathol. 2015;37(5):519-28. PubMed PMID: 26152639.

20. Prescott RJ, Freemont AJ, Jones CJ, Hoyland J, Fielding P. Sequential dermal microvascular and perivascular changes in the development of scleroderma. J Pathol. 1992;166(3):255-63. PubMed PMID: 1517881.

21. Distler JH, Akhmetshina A, Schett G, Distler O. Monocyte chemoattractant proteins in the pathogenesis of systemic sclerosis. Rheumatology (Oxford). 2009;48(2):98-103. PubMed PMID: 18984611.

22. Moroncini G, Svegliati Baroni S, Gabrielli A. Agonistic antibodies in systemic sclerosis. Immunol Lett. 2018;195:83-7. PubMed PMID: 29032187.

23. Orton SM, Peace-Brewer A, Schmitz JL, Freeman K, Miller WC, Folds JD. Practical evaluation of methods for detection and specificity of autoantibodies to extractable nuclear antigens. Clin Diagn Lab Immunol. 2004;11(2):297-301. PubMed PMID: 15013979.

24. Ho KT, Reveille JD. The clinical relevance of autoantibodies in scleroderma. Arthritis Res Ther. 2003;5(2):80-93. PubMed PMID: 12718748.

25. Hesselstrand R, Scheja A, Shen GQ, Wiik A, Akesson A. The association of antinuclear antibodies with organ involvement and survival in systemic sclerosis. Rheumatology (Oxford). 2003;42(4):534-40. PubMed PMID: 12649400.

26. Reveille JD, Solomon DH. Evidence-based guidelines for the use of immunologic tests: anticentromere, Scl-70, and nucleolar antibodies. Arthritis Rheum. 2003;49(3):399-412. PubMed PMID: 12794797.

27. Henault J, Robitaille G, Senecal JL, Raymond Y. DNA topoisomerase I binding to fibroblasts induces monocyte adhesion and activation in the presence of anti-topoisomerase I autoantibodies from systemic sclerosis patients. Arthritis Rheum. 2006;54(3):963-73. PubMed PMID: 16508979.

28. Kahaleh B, Matucci-Cerinic M. Raynaud's phenomenon and scleroderma. Dysregulated neuroendothelial control of vascular tone. Arthritis Rheum. 1995;38(1):1-4. PubMed PMID: 7818557.

29. Koenig M, Joyal F, Fritzler MJ, Roussin A, Abrahamowicz M, Boire G, et al. Autoantibodies and microvascular damage are independent predictive factors for the progression of Raynaud's phenomenon to systemic sclerosis: a twenty-year prospective study of 586 patients, with validation of proposed criteria for early systemic sclerosis. Arthritis Rheum. 2008;58(12):3902-12. PubMed PMID: 19035499.

30. Spencer-Green G. Outcomes in primary Raynaud phenomenon: a meta-analysis of the frequency, rates, and predictors of transition to secondary diseases. Arch Intern Med. 1998;158(6):595-600. PubMed PMID: 9521223.

31. Carvalho D, Savage CO, Black CM, Pearson JD. IgG antiendothelial cell autoantibodies from scleroderma patients induce leukocyte adhesion to human vascular endothelial cells in vitro. Induction of adhesion molecule expression and involvement of endothelium-derived cytokines. J Clin Invest. 1996;97(1):111-9. PubMed PMID: 8550821.

32. Salojin KV, Le Tonqueze M, Saraux A, Nassonov EL, Dueymes M, Piette JC, et al. Antiendothelial cell antibodies: useful markers of systemic sclerosis. Am J Med. 1997;102(2):178-85. PubMed PMID: 9217568.

33. Avouac J, Fransen J, Walker UA, Riccieri V, Smith V, Muller C, et al. Preliminary criteria for the very early diagnosis of systemic sclerosis: results of a Delphi Consensus Study from EULAR Scleroderma Trials and Research Group. Ann Rheum Dis. 2011;70(3):476-81. PubMed PMID: 21081523.

34. Tashkin DP, Elashoff R, Clements PJ, Goldin J, Roth MD, Furst DE, et al. Cyclophosphamide versus placebo in scleroderma lung disease. N Engl J Med. 2006;354(25):2655-66. PubMed PMID: 16790698.

35. Beyer C, Distler O, Distler JH. Innovative antifibrotic therapies in systemic sclerosis. Curr Opin Rheumatol. 2012;24(3):274-80. PubMed PMID: 22450392.

36. Ramos-Casals M, Fonollosa-Pla V, Brito-Zeron P, Siso-Almirall A. Targeted therapy for systemic sclerosis: how close are we? Nat Rev Rheumatol. 2010;6(5):269-78. PubMed PMID: 20386562.

37. Klinkhammer BM, Floege J, Boor P. PDGF in organ fibrosis. Mol Aspects Med. 2018;62:44-62. PubMed PMID: 29155002.

38. Heldin CH, Westermark B. Mechanism of action and in vivo role of platelet-derived growth factor. Physiol Rev. 1999;79(4):1283-316. PubMed PMID: 10508235.

39. Trojanowska M. Role of PDGF in fibrotic diseases and systemic sclerosis. Rheumatology (Oxford). 2008;47 Suppl 5:v2-4. PubMed PMID: 18784131.

40. Olson LE, Soriano P. Increased PDGFRalpha activation disrupts connective tissue development and drives systemic fibrosis. Dev Cell. 2009;16(2):303-13. PubMed PMID: 19217431.

41. Kazlauskas A. PDGFs and their receptors. Gene. 2017;614:1-7. PubMed PMID: 28267575.

42. Svegliati S, Cancello R, Sambo P, Luchetti M, Paroncini P, Orlandini G, et al. Platelet-derived growth factor and reactive oxygen species (ROS) regulate Ras protein levels in primary human fibroblasts via ERK1/2. Amplification of ROS and Ras in systemic sclerosis fibroblasts. J Biol Chem. 2005;280(43):36474-82. PubMed PMID: 16081426.

43. Baroni SS, Santillo M, Bevilacqua F, Luchetti M, Spadoni T, Mancini M, et al. Stimulatory autoantibodies to the PDGF receptor in systemic sclerosis. N Engl J Med. 2006;354(25):2667-76. PubMed PMID: 16790699.

44. Yamakage A, Kikuchi K, Smith EA, LeRoy EC, Trojanowska M. Selective upregulation of platelet-derived growth factor alpha receptors by transforming growth factor beta in scleroderma fibroblasts. J Exp Med. 1992;175(5):1227-34. PubMed PMID: 1314885.

45. Gallini R, Lindblom P, Bondjers C, Betsholtz C, Andrae J. PDGF-A and PDGF-B induces cardiac fibrosis in transgenic mice. Exp Cell Res. 2016;349(2):282-90. PubMed PMID: 27816607.

46. Mueller AA, van Velthoven CT, Fukumoto KD, Cheung TH, Rando TA. Intronic polyadenylation of PDGFRalpha in resident stem cells attenuates muscle fibrosis. Nature. 2016;540(7632):276-9. PubMed PMID: 27894125.

47. Gabrielli A, Svegliati S, Moroncini G, Avvedimento EV. Pathogenic autoantibodies in systemic sclerosis. Curr Opin Immunol. 2007;19(6):640-5. PubMed PMID: 18083509.

48. Moroncini G et al, World Biomedical Frontiers, Arthitis 2015. ISSN: 2328-0166

49. Moroncini G, Cuccioloni M, Mozzicafreddo M, Pozniak KN, Grieco A, Paolini C, et al. Characterization of binding and quantification of human autoantibodies to PDGFRalpha using a biosensor-based approach. Anal Biochem. 2017;528:26-33. PubMed PMID: 28450104.

50. Fraticelli P, De Vita S, Franzolini N, Svegliati S, Scott CA, Tonnini C, et al. Reduced type I collagen gene expression by skin fibroblasts of patients with systemic sclerosis after one treatment course with rituximab. Clin Exp Rheumatol. 2015;33(4 Suppl 91):S160-7. PubMed PMID: 26339895.

51. Svegliati S, Amico D, Spadoni T, Fischetti C, Finke D, Moroncini G, et al. Agonistic Anti-PDGF Receptor Autoantibodies from Patients with Systemic Sclerosis Impact Human

Pulmonary Artery Smooth Muscle Cells Function In Vitro. Front Immunol. 2017;8:75. PubMed PMID: 28228756.

52. Yue X, Yu X, Petersen F, Riemekasten G. Recent advances in mouse models for systemic sclerosis. Autoimmun Rev. 2018;17(12):1225-34. PubMed PMID: 30316997.

53. Marangoni RG, Varga J, Tourtellotte WG. Animal models of scleroderma: recent progress. Curr Opin Rheumatol. 2016;28(6):561-70. PubMed PMID: 27533324.

54. Manetti M, Rosa I, Milia AF, Guiducci S, Carmeliet P, Ibba-Manneschi L, et al. Inactivation of urokinase-type plasminogen activator receptor (uPAR) gene induces dermal and pulmonary fibrosis and peripheral microvasculopathy in mice: a new model of experimental scleroderma? Ann Rheum Dis. 2014;73(9):1700-9. PubMed PMID: 23852693.

55. Asano Y, Sato S. Animal models of scleroderma: current state and recent development. Curr Rheumatol Rep. 2013;15(12):382. PubMed PMID: 24150871.

56. Beyer C, Schett G, Distler O, Distler JH. Animal models of systemic sclerosis: prospects and limitations. Arthritis Rheum. 2010;62(10):2831-44. PubMed PMID: 20617524.

57. Wei J, Melichian D, Komura K, Hinchcliff M, Lam AP, Lafyatis R, et al. Canonical Wnt signaling induces skin fibrosis and subcutaneous lipoatrophy: a novel mouse model for scleroderma? Arthritis Rheum. 2011;63(6):1707-17. PubMed PMID: 21370225.

58. Moroncini G, Paolini C, Orlando F, Capelli C, Grieco A, Tonnini C, et al. Mesenchymal stromal cells from human umbilical cord prevent the development of lung fibrosis in immunocompetent mice. PLoS One. 2018;13(6):e0196048. PubMed PMID: 29856737.

59. Orlando F, Paolini C, Agarbati S, Tonnini C, Grieco A, Capelli C, et al. Induction of Mouse Lung Injury by Endotracheal Injection of Bleomycin. J Vis Exp. 2019;(146). PubMed PMID: 31107440.

60. Soare A, Ramming A, Avouac J, Distler JHW. Updates on animal models of systemic sclerosis. Journal of Scleroderma and Related Disorders. 2016;1(3):266-76. PubMed PMID: ISI:000404600200005.

61. Hohenstein P, Slight J, Ozdemir DD, Burn SF, Berry R, Hastie ND. High-efficiency Rosa26 knock-in vector construction for Cre-regulated overexpression and RNAi. Pathogenetics. 2008;1(1):3. PubMed PMID: 19014667.

62. Malavolta M, Basso A, Piacenza F, Giacconi R, Costarelli L, Pierpaoli S, et al. Survival study of metallothionein-1 transgenic mice and respective controls (C57BL/6J): influence of a zinc-enriched environment. Rejuvenation Res. 2012;15(2):140-3. PubMed PMID: 22533418.

63. Kadota Y, Aki Y, Toriuchi Y, Mizuno Y, Kawakami T, Sato M, et al. Deficiency of metallothionein-1 and -2 genes shortens the lifespan of the 129/Sv mouse strain. Exp Gerontol. 2015;66:21-4. PubMed PMID: 25871729.

64. Abzazou T, Salvado H, Cardenas-Youngs Y, Becerril-Rodriguez A, Cebiran EMC, Huguet A, et al. Characterization of nutrient-removing microbial communities in two full-scale WWTP

systems using a new qPCR approach. Sci Total Environ. 2018;618:858-65. PubMed PMID: 29054664.

65. Whelan JA, Russell NB, Whelan MA. A method for the absolute quantification of cDNA using real-time PCR. J Immunol Methods. 2003;278(1-2):261-9. PubMed PMID: 12957413.

66. Wermuth PJ, Mendoza FA, Jimenez SA. Abrogation of transforming growth factor-beta-induced tissue fibrosis in mice with a global genetic deletion of Nox4. Lab Invest. 2018;99(4):470-82. PubMed PMID: 30470772.

67. Markova MS, Zeskand J, McEntee B, Rothstein J, Jimenez SA, Siracusa LD. A role for the androgen receptor in collagen content of the skin. J Invest Dermatol. 2004;123(6):1052-6. PubMed PMID: 15610513.

68. Manne J, Markova M, Siracusa LD, Jimenez SA. Collagen content in skin and internal organs of the tight skin mouse: an animal model of scleroderma. Biochem Res Int. 2013;2013:436053. PubMed PMID: 24260716.

69. Montironi R, Cheng L, Mazzucchelli R, Morichetti D, Stramazzotti D, Santinelli A, et al. Immunohistochemical detection and localization of somatostatin receptor subtypes in prostate tissue from patients with bladder outlet obstruction. Cell Oncol. 2008;30(6):473-82. PubMed PMID: 18936524.

70. Flurkey K, M. Currer J, Harrison DE, Fox JG, Davisson MT, Quimby FW, et al. Chapter 20 - Mouse Models in Aging Research. The Mouse in Biomedical Research (Second Edition). Burlington: Academic Press; 2007. p. 637-72.

71. Liang M, Lv J, Zou L, Yang W, Xiong Y, Chen X, et al. A modified murine model of systemic sclerosis: bleomycin given by pump infusion induced skin and pulmonary inflammation and fibrosis. Lab Invest. 2015;95(3):342-50. PubMed PMID: 25502178.

72. Kliment CR, Englert JM, Crum LP, Oury TD. A novel method for accurate collagen and biochemical assessment of pulmonary tissue utilizing one animal. Int J Clin Exp Pathol. 2011;4(4):349-55. PubMed PMID: 21577320.